

Clustering of solutions in the symmetric binary perceptron

Carlo Baldassi,^{1,2} Riccardo Della Vecchia,¹ Carlo Lucibello,¹ and Riccardo Zecchina^{1,3}

¹*Artificial Intelligence Lab, Institute for Data Science and Analytics, Bocconi University, Milano, Italy*

²*Istituto Nazionale di Fisica Nucleare, Sezione di Torino, Italy*

³*International Centre for Theoretical Physics, Trieste, Italy*

The geometrical features of the (non-convex) loss landscape of neural network models are crucial in ensuring successful optimization and, most importantly, the capability to generalize well. While minimizers' flatness consistently correlates with good generalization, there has been little rigorous work in exploring the condition of existence of such minimizers, even in toy models. Here we consider a simple neural network model, the symmetric perceptron, with binary weights. Phrasing the learning problem as a constraint satisfaction problem, the analogous of a flat minimizer becomes a large and dense cluster of solutions, while the narrowest minimizers are isolated solutions. We perform the first steps toward the rigorous proof of the existence of a dense cluster in certain regimes of the parameters, by computing the first and second moment upper bounds for the existence of pairs of arbitrarily close solutions. Moreover, we present a non rigorous derivation of the same bounds for sets of y solutions at fixed pairwise distances.

I. INTRODUCTION

The problem of learning to classify a set random patterns with a *binary perceptron* has been a recurrent topic since the very beginning of the statistical physics studies of neural networks models [1]. The learning problem consists in finding the optimal binary assignments of the connection weights which minimize the number of misclassifications of the patterns. We shall refer to such set of optimal assignments as the space of solutions of the perceptron. In spite of the extremely simple architecture of the model, the learning task is highly non convex and its geometrical features are believed to play a role also in more complex neural architectures [2–4].

For the case of random i.i.d. patterns, the space of solutions of the binary perceptron is known to be dominated by an exponential number of isolated solutions [5] which lie at a large mutual Hamming distances [6, 7] (golf course landscape). An even larger number of local minima have been shown to exist [?].

The study of how the number of these isolated solutions decreases as more patterns are learned provides the correct prediction for the so-called capacity of the binary perceptron, i.e. the maximum number of random patterns that can be correctly classified. However, the same analysis does not provide the insight necessary for understanding the behavior of learning algorithms: one would expect that finding solutions in a golf course landscape should be difficult for search algorithms, and indeed Monte Carlo based algorithms satisfying detailed balance get stuck in local minima; yet, empirical results have shown that many learning algorithms, even simple ones, are able to find solutions efficiently [8–11].

These empirical results suggested that the solutions which were not the dominant ones in the Gibbs measure, and were as such neglected in the analysis of the capacity, could in fact play an important algorithmic role. As discussed in refs. [12, 13] this turned out to be the actual case: the study of the dominant solutions in the Gibbs measure theory does not take into account the existence of rare (sub-dominant) regions in the solution space which are those found by algorithms. Revealing those rare, accessible regions required a large deviation analysis based on the notion of *local entropy*, which is a measure of the density of solutions in an extensive region of the configuration space (see the precise definition in the next section). The regions of maximal local entropy are extremely dense in solutions, such that (for finite N) nearly every configuration in the region is a solution. More recently, the existence of high local entropy / flat regions has been found also in multi-layer networks with continuous weights, and their role has been connected to the structural characteristics of deep neural networks [15?].

All the above results rely on methods of statistical mechanics of disordered systems which are extremely powerful and yet not fully rigorous. It is therefore important to corroborate them with rigorous bounds [16]. In a recent paper [17], Aubin et al. have studied a simple variant of the binary perceptron model for which the rigorous bounds provided by first and second moment methods can be shown to be tight. The authors have been able to confirm the predictions of the statistical physics

methods concerning the capacity of the model, and the golf course nature of the space of solutions. The model that the authors have studied has a modified activation criterion compared to the traditional perceptron, replacing the Heaviside step function by a function with an even symmetry.

The goal of the present paper is to study the existence of dense regions in the the symmetrized binary perceptron model. In sec. II we define the model and, as a preliminary step, we present the results of the replica-method large deviation analysis, which predicts that the phenomenology for the symmetrized model is the same as for the traditional one, and thus that high local entropy regions exist. If these predictions are correct, then it should be possible, at least for some range of the parameters, to choose any integer number $y \geq 2$ and find a threshold $x_c(y)$ such that for any $x < x_c(y)$ there is an exponential number of groups of y solutions all at mutual Hamming distance $\lfloor Nx \rfloor$. In the remainder of the paper we try to verify this statement, by employing the first and second moment methods where possible. In sec. III we address the $y = 2$ case: we extend the analysis of ref. [17] and show rigorously (except for a numerical optimization step) that, for small enough constraint density α , there exist an exponential number of pairs of solutions at arbitrary $O(N)$ Hamming distance. In sec. IV we study the general y case. For $y = 3$ or 4 , we can derive a rigorous upper bound that coincides with the non-rigorous results for general y . As for the lower bound, only the $y = 2$ case can be derived rigorously (and again it coincides with the non-rigorous results that we also derive). All the results are thus consistent with the existence of high local entropy regions, as predicted by the large deviation study.

II. DENSE CLUSTERS IN THE SYMMETRIC BINARY PERCEPTRON

A. Model definition

We investigate the rectangular-binary-perceptron (RBP) problem introduced in ref. [17]. The RBP has the key property of having a symmetric activation function, characterized by a parameter $K > 0$. Given a vector of binary weights $\mathbf{w} \in \{\pm 1\}^N$ and an input $\xi \in \mathbb{R}^N$ (an example), we say that \mathbf{w} satisfies the example if $|\xi \cdot \mathbf{w}| < K$.¹ This symmetry simplifies the theoretical analysis and allows to obtain tighter bounds for the storage capacity through the first and second moment methods.

For a given set of inputs $\xi^\mu \in \mathbb{R}^N$, with $\mu = 1, \dots, M$, the RBP problem can be expressed as a constraint satisfaction problem (CSP) over the binary weights. Throughout the paper we will assume the entries ξ_i^μ to be *i.i.d.* Gaussian variables with zero mean and variance $1/N$. A binary vector $\mathbf{w} \in \{\pm 1\}^N$ is called a *solution* of the problem if it satisfies

$$\sum_{i=1}^N w_i \xi_i^\mu \in I_K \quad \forall \mu \in [M], \quad (1)$$

where $I_K = [-K, K]$. Equivalently, a vector \mathbf{w} is a solution of the RBP problem iff the function $\mathbb{X}_{\xi, K} : \{-1, 1\}^N \rightarrow \{0, 1\}$, defined as

$$\mathbb{X}_{\xi, K}(\mathbf{w}) = \prod_{\mu=1}^M \mathbb{1} \left(\sum_{i=1}^N w_i \xi_i^\mu \in I_K \right), \quad (2)$$

is equal to one, where we have denoted with $\mathbb{1}(p)$ an indicator function that is 1 if the statement p is true and 0 otherwise.

The *storage capacity* is then defined similarly to the satisfiability threshold in random constraint satisfaction problems: we denote the constraint density as $\alpha \equiv M/N$ and define the storage capacity $\alpha_c(K)$, also known as SAT-UNSAT transition point,

¹ This setting corresponds to a binary classification problem with training examples from a single class. This simplifies the analysis.

as the infimum of densities α such that, in the limit $N \rightarrow \infty$, with high probability (over the choice of the matrix ξ_i^μ) there are no solutions. It is natural to conjecture that the converse also holds, i.e. that the storage capacity $\alpha_c(K)$ equals the supremum of α such that in the limit $N \rightarrow \infty$ solutions exist with high probability. In this case we would say the storage capacity is a *sharp threshold*.

B. Replicated Systems and Dense Clusters

In order to obtain a geometric characterization of the solution space, we consider the Hamming distance of any two configurations \mathbf{w}^1 and \mathbf{w}^2 , defined by

$$d_H(\mathbf{w}^1, \mathbf{w}^2) \equiv \sum_{i=1}^N (1 - w_i^1 w_i^2) / 2.$$

Even if an exponential number of solutions exist for $\alpha < \alpha_c(K)$, the overwhelming majority are *isolated*: for each such solution, there exists a radius r_{\min} such that the number of other solutions within a distance $\lfloor Nr_{\min} \rfloor$ is sub-exponential. We are interested instead in the presence of *dense regions*, which are characterized by the fact that there is a configuration around which the number of solutions within a given radius $\lfloor Nr \rfloor$ is exponential for all r in some neighborhood of 0. We speak of *ultra-dense* regions when the logarithm of the density of solutions tends exponentially fast to 0 as $r \rightarrow 0$.

Suppose now that a dense region around some reference configuration exists, choose a sufficiently small value $r > 0$, and call x the typical distance between any two solutions at distance r from the reference. In general, $0 < x \leq 2r$, and for an ultra-dense region $x = 2r(1 - r)$ in the limit of large N . Therefore for any x below some threshold there should exist an exponential number of solutions at mutual normalized distance x .

We thus investigate the problem of finding a set of y solutions of the RBP problem, where y is an arbitrary natural number, with all pairwise distances constrained to some value $\lfloor Nx \rfloor$. The existence (for some range of α) of such set of solutions, w.h.p. in the large N limit, for arbitrarily large values of y and all x in some neighborhood of 0, is a necessary condition for the presence of dense regions. These sets of y solutions would coexist with an exponentially larger number of isolated solutions, and therefore the usual tools of statistical physics are not sufficient to reveal their presence, and a large deviation analysis is necessary [12].

As a starting point for the analysis we introduce the partition function of the model with y real replicas, \mathcal{Z}_y , accounting for the number of such sets (up to a $y!$ symmetry factor). For any fixed (normalized) distance $x \in [0, 1]$, this is given by

$$\mathcal{Z}_y(x, K, \xi) \equiv \sum_{\{\mathbf{w}^a\}_{a=1}^y} \prod_{a=1}^y \mathbb{X}_{\xi, K}(\mathbf{w}^a) \prod_{a < b}^y \mathbb{1}(d_H(\mathbf{w}^a, \mathbf{w}^b) = \lfloor Nx \rfloor). \quad (3)$$

The summation here is over the 2^{yN} spin configurations. We denote with $\alpha_c^y(x, K)$ the SAT/UNSAT threshold (if it exists) in the $N \uparrow \infty$ limit and under the probability distribution for ξ described in the previous Section. The asymptotic behavior is captured by the (normalized) local entropy ϕ_y defined by²

$$\phi_y(x, K, \alpha) = \lim_{N \rightarrow \infty} \frac{1}{yN} \mathbb{E}_\xi \ln \mathcal{Z}_y(x, K, \xi). \quad (4)$$

² We use a simpler definition compared to ref. [12] here, avoiding the explicit use of a reference configuration. The technical justification for this can be found in ref. [?]; intuitively, the reference is defined implicitly as the barycenter, and the results are basically equivalent for large y .

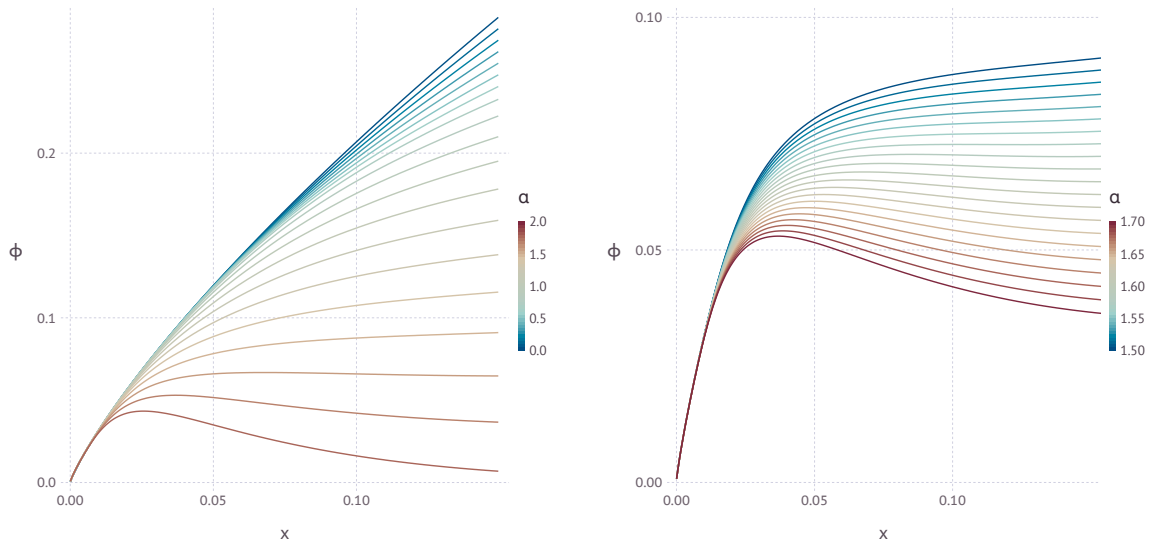


Figure 1. Plot of free local entropy of eq. (3) as a function of the normalized Hamming distance between solutions x , obtained with the replica method using the replica-symmetric ansatz (see Appendix A for the details). In both figures the value of the half-width of the channel is $K = 1$. (Left) Curves for $\alpha = 0$ up to $\alpha = 1.8$ in steps of 0.1. When the distance x approaches zero we see that all curves tend to coincide with the curve for $\alpha = 0$, meaning that there exist regions of solutions that are maximally dense (nearly all configurations are solutions) in their immediate surroundings. (Right) Zoom on the interval of values of α where there is a change in monotonicity, which we interpret as signaling a fragmentation of the dense clusters into separate pieces. We refine the step of α to 0.01, and we find that the change happens for $\alpha_U \simeq 1.58$.

The interpretation of this quantity is as follows. If ϕ_y is positive, the number of groups of y solutions is exponential. For any group of y solutions that contributes to the sum in \mathcal{Z}_y we can use their barycenter (which will be at distance $r = \frac{1-\sqrt{1-2x}}{2}$ from each of them) as a reference configuration, and in the limit of large y the sum is dominated by the regions with the highest density of solutions at distance r from their center, provided they are evenly distributed. Also in this limit the logarithm of the density of solutions is computed as $\phi_y(x, K, \alpha) - \phi_y(x, K, 0) = \phi_y(x, K, \alpha) - H_2\left(\frac{1-\sqrt{1-2x}}{2}\right)$ where $H_2(r) = -r \ln r - (1-r) \ln(1-r)$ is the two-state entropy function. If a dense region exists around a configuration, we should observe a positive ϕ_y for all y and for all x in some neighborhood of 0, and for ultra-dense regions we should have $\lim_{y \rightarrow \infty} \phi_y(x, K, \alpha) = H_2\left(\frac{1-\sqrt{1-2x}}{2}\right) - O\left(e^{-\frac{1}{x}}\right)$ for sufficiently small x .³

The computation of ϕ_y can be approached by rigorous techniques only for small y , as discussed in the next sections. In the general case, for any finite y and in the $y \rightarrow \infty$ limit, it can be carried out at present only using the non-rigorous replica method of statistical physics of disordered systems. The computations for this model follow entirely those of ref. [12] and are reported in Appendix A.

The replica analysis in the $y \rightarrow \infty$ limit strongly suggests the existence of ultra-dense regions of solutions: as shown in fig. 1, for $K = 1$ and for sufficiently small x the curves for α below the SAT-UNSAT transition, i.e. $\alpha < \alpha_c \simeq 1.815 \dots$, tend

³ Although these are in principle necessary conditions, and not sufficient, the latter scenario of a log-density going to 0 in particular seems very unlikely in the absence of ultra-dense regions, and indeed when the matter was investigated numerically for the standard perceptron model these rare regions were found and their properties were in good agreement with the theory in a wide range of parameters [12, 13].

to collapse onto the curve for $\alpha = 0$, implying that these regions are maximally dense in their immediate surroundings (nearly all configurations are solutions in an extensive region centered around their barycenter). Furthermore, there is a transition at around $\alpha_U \simeq 1.58$ after which the curves are no longer monotonic. Overall, this is the same phenomenology that was observed (and confirmed by numerical simulations) for the standard binary perceptron model in ref. [12], and we interpret it in the same way, i.e. we speculate that ultra-dense sub-dominant regions of solutions exist, and that the break of monotonicity at $\alpha_U \simeq 1.58$ signals a transition⁴ between two regimes: one for low α in which the ultra-dense regions are immersed in a vast connected structure, and one at high α in which the structure of the dense solutions fragments into separate regions that are no longer easily accessible.⁵

These results were obtained with the so-called replica-symmetric ansatz, and they are certainly not exact. However, as in previous studies [12], the corrections (which would require the use of a replica-symmetry-broken ansatz) only become numerically relevant at relatively large α (e.g. we may expect small corrections to the value of α_U , and larger effects close to α_c), and they don't affect the qualitative picture, the emerging phenomenology and its physical interpretation.

III. PAIRS OF SOLUTIONS ($y = 2$): RIGOROUS BOUNDS

We are able to derive rigorous lower and upper bounds for the existence of pairs of solutions, i.e. for the $y = 2$ case, without resorting to the replica method.

The idea of the derivation follows very closely the strategy used in refs. [18, 19] for the random K-SAT problem.

We define a SAT- x -pair as a pair of binary weights $\mathbf{w}^1, \mathbf{w}^2 \in \{-1, 1\}^N$, which are both solutions of the CSP, and whose Hamming distance is $d_H(\mathbf{w}^1, \mathbf{w}^2) = \lfloor Nx \rfloor$. The number of such pairs is $\mathcal{Z}_{y=2}(x, K, \xi)$, see eq. (3).

A. Upper bound: the first moment method

In this section we are interested in finding an upper-bound (which depends on x) to the critical capacity of pairs of solutions. To do that we use the upper bound $\mathbb{P}[X > 0] \leq \mathbb{E}[X]$ that holds when the random variable X is non-negative and integer-valued. When we apply it to the random variable $\mathcal{Z}_{y=2}$ we get:

$$\mathbb{P}[\mathcal{Z}_{y=2}(x, K, \xi) > 0] \leq \mathbb{E}[\mathcal{Z}_{y=2}(x, K, \xi)] = 2^N \binom{N}{\lfloor Nx \rfloor} \mathbb{P}[v_1 \in I_K, v_2 \in I_K]^M \quad (5)$$

where we have introduced the two Gaussian random variables v_1 and v_2 , with $\mathbb{E}[v_1] = \mathbb{E}[v_2] = 0$, $\mathbb{E}[v_1^2] = \mathbb{E}[v_2^2] = 1$, and covariance

$$\mathbb{E}[v_1 v_2] = \frac{N - 2 \lfloor Nx \rfloor}{N} \xrightarrow{N \rightarrow +\infty} 1 - 2x. \quad (6)$$

Let us consider the normalized logarithm of the first moment,

$$F(x, K, \alpha) = \lim_{N \rightarrow \infty} \frac{1}{N} \ln \mathbb{E}[\mathcal{Z}_{y=2}(x, K, \xi)] = \ln 2 + H_2(x) + \alpha \ln f_1(x, K), \quad (7)$$

⁴ In ref. [12] it was shown that some geometric constraints are violated in a region of x for $\alpha \geq \alpha_U$ implying the onset of strong symmetry-breaking effects, with numerical evidence supporting the switch to a different regime.

⁵ It should be noted that in the standard binary perceptron case (i.e. with sign activation) there is empirical evidence only for the first scenario of a vast connected structure with ultra-dense regions in it, while the second scenario of fragmented regions has never been directly observed at large N , arguably due to the intrinsic algorithmic hardness of finding such regions.

where as before $H_2(x) = -x \ln x - (1-x) \ln(1-x)$ is the two-state entropy function while $f_1(x, K)$ is defined as follows. Denote with Σ_2 the covariance matrix of the Gaussian random vector $\vec{v} = (v_1, v_2)$ whose components have covariance equal to $1 - 2x$ and variances equal to one. We define $f_1(x, K)$ as the probability that this random vector takes values in the box $[-K, K]^2$:

$$\begin{aligned} f_1(x, K) &= \frac{1}{2\pi |\Sigma_2|^{1/2}} \int_{-K}^K \int_{-K}^K dv_1 dv_2 e^{-\vec{v}^T \Sigma_2^{-1} \vec{v}} \\ &= \int_{-K}^K du_1 \frac{e^{-u_1^2/2}}{\sqrt{2\pi}} \int_{\frac{-K-(1-2x)u_1}{2\sqrt{x(1-x)}}}^{\frac{K-(1-2x)u_1}{2\sqrt{x(1-x)}}} du_2 \frac{e^{-u_2^2/2}}{\sqrt{2\pi}}. \end{aligned} \quad (8)$$

From the inequality (5), $F(x, K, \alpha) < 0$ implies that $\lim_{N \rightarrow \infty} \mathbb{P}[\mathcal{Z}_{y=2}(x, K, \xi) > 0] = 0$. In turn this provides the upper bound we are seeking:

Upper Bound. For each K and $0 < x < 1$, and for all α such that

$$\alpha > \alpha_{UB}(x, K) \equiv -\frac{\ln 2 + H_2(x)}{\ln f_1(x, K)} \quad (9)$$

there are no SAT- x -pairs w.h.p.

Notice that the first moment computation for $\mathcal{Z}_{y=2}(x)$ is similar to the second moment computation for $\mathcal{Z}_{y=1}$ in ref. [17]: in the former x enters as an external constraint, in the latter as an order parameter to be optimized.

The upper bound that we obtained for $K = 1$ and as a function of x is shown in fig. 2. For $x = 0$ the upper bound trivially reduces to the one for a single replica as found in ref. [17]. The same happens also for $x = 1/2$, as the two constrained replicas behave as independent systems in the large N limit.

B. Lower bound: the second moment method

We compute the lower bound to the critical capacity using the second moment method, which is a direct consequence of the Cauchy-Schwarz inequality:

Lemma 1 (Second moment method). *If X is a non-negative random variable, then*

$$\mathbb{P}[X > 0] \geq \frac{\mathbb{E}[X]^2}{\mathbb{E}[X^2]}. \quad (10)$$

From the results of section III A we have

$$\mathbb{E}[\mathcal{Z}_{y=2}(x, K, \xi)] = 2^N \binom{N}{\lfloor Nx \rfloor} f_1\left(\frac{\lfloor Nx \rfloor}{N}, K\right)^M, \quad (11)$$

where $f_1(x, K)$ is defined like in eq. (8). The second moment of the random variable $\mathcal{Z}_{y=2}$ follows from simple combinatorics and reads

$$\begin{aligned}
\mathbb{E} \left[\mathcal{Z}_{y=2}^2(x, K, \xi) \right] &= \sum_{\{\mathbf{w}^1\}} \sum_{\{\mathbf{w}^2\}} \sum_{\{\tilde{\mathbf{w}}^1\}} \sum_{\{\tilde{\mathbf{w}}^2\}} \mathbb{1} \left(d_H(\mathbf{w}^1, \mathbf{w}^2) = \lfloor Nx \rfloor \right) \mathbb{1} \left(d_H(\tilde{\mathbf{w}}^1, \tilde{\mathbf{w}}^2) = \lfloor Nx \rfloor \right) \times \\
&\quad \times \prod_{\mu=1}^M \mathbb{E} \left[\mathbb{1} \left(w^1 \cdot \xi^\mu \in I_K \right) \mathbb{1} \left(w^2 \cdot \xi^\mu \in I_K \right) \mathbb{1} \left(\tilde{w}^1 \cdot \xi^\mu \in I_K \right) \mathbb{1} \left(\tilde{w}^2 \cdot \xi^\mu \in I_K \right) \right] \quad (12) \\
&= 2^N \sum_{\mathbf{a} \in V_{N,x} \cap \{0, 1/N, 2/N, \dots, 1\}^8} \frac{N!}{\prod_{i=0}^7 (Na_i)!} f_2(\mathbf{a}, x, K)^M,
\end{aligned}$$

where we have adopted the following conventions.

- \mathbf{a} is an 8-component vector giving the proportion of each type of quadruplets $(w_i^1, w_i^2, \tilde{w}_i^1, \tilde{w}_i^2)$ as described in the table below, where we have arbitrarily (but without loss of generality) fixed \mathbf{w}^1 to $(1, \dots, 1)$. Fixing the vector \mathbf{a} entails fixing all the possible overlaps between the vectors w^1, w^2, \tilde{w}^1 and \tilde{w}^2 and consequently the covariances of the random variables $z_1 := w^1 \cdot \xi$, $z_2 := w^2 \cdot \xi$, $\tilde{z}_1 := \tilde{w}^1 \cdot \xi$ and $\tilde{z}_2 := \tilde{w}^2 \cdot \xi$ with $\xi_i \sim \mathcal{N}(0, 1/N)$ i.i.d. These covariances as functions of \mathbf{a} are made explicit in eq. (13).

	a_0	a_1	a_2	a_3	a_4	a_5	a_6	a_7
w_i^1	+	+	+	+	+	+	+	+
w_i^2	+	+	+	+	-	-	-	-
\tilde{w}_i^1	+	+	-	-	+	+	-	-
\tilde{w}_i^2	+	-	+	-	+	-	+	-

- $f_2(\mathbf{a}, x, K)$ has the expression

$$f_2(\mathbf{a}, x, K) = \mathbb{P}[z_1 \in I_K, z_2 \in I_K, \tilde{z}_1 \in I_K, \tilde{z}_2 \in I_K].$$

where $\mathbf{z}^T := (z_1, z_2, \tilde{z}_1, \tilde{z}_2)$ is a 4-dimensional Gaussian vector, with the following set of covariances:

$$\Sigma = \begin{pmatrix} 1 & q_1 & q_{01} & q_{02} \\ q_1 & 1 & q_{03} & q_{04} \\ q_{01} & q_{03} & 1 & q_1 \\ q_{02} & q_{04} & q_1 & 1 \end{pmatrix} \quad \text{where} \quad \begin{cases} q_1 = 1 - 2 \frac{\lfloor Nx \rfloor}{N} \\ q_{01} = 1 - 2(a_2 + a_3 + a_6 + a_7) \\ q_{02} = 1 - 2(a_1 + a_3 + a_5 + a_7) \\ q_{03} = 1 - 2(a_2 + a_3 + a_4 + a_5) \\ q_{04} = 1 - 2(a_1 + a_3 + a_4 + a_6) \end{cases}. \quad (13)$$

Therefore $f_2(\mathbf{a}, x, K)$ can be simply written as the following Gaussian integral

$$f_2(\mathbf{a}, x, K) = \int_{I_K^4} dz_1 dz_2 d\tilde{z}_1 d\tilde{z}_2 \frac{1}{(2\pi)^2 |\Sigma|^{1/2}} e^{-\frac{1}{2} \mathbf{z}^T \Sigma^{-1} \mathbf{z}}. \quad (14)$$

- The set $V_{N,x} \subset [0, 1]^8$ is a simplex specified by:

$$\begin{cases} \lfloor N(a_4 + a_5 + a_6 + a_7) \rfloor = \lfloor Nx \rfloor \\ \lfloor N(a_1 + a_2 + a_5 + a_6) \rfloor = \lfloor Nx \rfloor \\ \sum_{i=0}^7 a_i = 1 \end{cases}. \quad (15)$$

These three conditions correspond to the normalization of the proportions and to the enforcement of the conditions $d_{\mathbf{w}^1 \mathbf{w}^2} = \lfloor Nx \rfloor$, $d_{\tilde{\mathbf{w}}^1 \tilde{\mathbf{w}}^2} = \lfloor Nx \rfloor$. When $N \rightarrow \infty$, $V_x = \bigcap_{N \in \mathbb{N}} V_{N,x}$ defines a five-dimensional simplex described by the three hyperplanes:

$$\begin{cases} a_4 + a_5 + a_6 + a_7 = x \\ a_1 + a_2 + a_5 + a_6 = x \\ \sum_{i=0}^7 a_i = 1 \end{cases} \quad (16)$$

In order to yield an asymptotic estimate of $\mathbb{E} \left[\mathcal{Z}_{y=2}^2 \right]$ we first use the following known result, which comes from the approximation of integrals by sums (proof in Appendix B 2):

Lemma 2. *Let $\psi(\mathbf{a})$ be a real, positive, continuous function of \mathbf{a} , and let $V_{N,x}$, V_x be as defined above. Then for any given x there exists a constant C_0 such that for sufficiently large N :*⁶

$$\sum_{\mathbf{a} \in V_{N,x} \cap \{0,1/N,2/N,\dots,1\}^8} \frac{N!}{\prod_{i=0}^7 (Na_i)!} \psi(\mathbf{a})^N \leq C_0 N^{3/2} \int_{V_x} d\mathbf{a} e^{N[H_8(\mathbf{a}) + \ln \psi(\mathbf{a})]}, \quad (17)$$

where $H_8(\mathbf{a}) = -\sum_{i=0}^7 a_i \ln a_i$.

The bound for the second moment then reads:

$$\mathbb{E} \left[\mathcal{Z}_{y=2}^2(x, K, \xi) \right] \leq C_0 N^{3/2} \int_{V_x} d\mathbf{a} e^{N[\ln 2 + H_8(\mathbf{a}) + \alpha \ln f_2(\mathbf{a}, x, K)]}, \quad (18)$$

which is obtained from substitution of eq. (12) into Lemma 2. The number of components of the vector \mathbf{a} is eight, but we can reduce their number to five with a change of variables and rewrite the integral in a particularly simple form where f_2 just depends on four of them. This is done in Appendix B 1. Here we give just the final expression where the new integration variables are η (a scalar) and $\vec{q}_0 = (q_{01}, q_{02}, q_{03}, q_{04})$. The bound becomes

$$\mathbb{E} \left[\mathcal{Z}_{y=2}^2(x, K, \xi) \right] \leq C_0 N^{3/2} \int_{\tilde{V}_x} d\vec{q}_0 d\eta e^{N[\ln 2 + H_8(\vec{q}_0, \eta, x) + \alpha \ln f_2(\vec{q}_0, x, K)]}, \quad (19)$$

where:

- $f_2(\vec{q}_0, x, K)$ has the expression

$$f_2(\vec{q}_0, x, K) = \int_{I_K^4} dz_1 dz_2 d\tilde{z}_1 d\tilde{z}_2 \frac{1}{(2\pi)^2 |\Sigma|^{1/2}} e^{-\frac{1}{2} \mathbf{z}^T \Sigma^{-1} \mathbf{z}},$$

where Σ is the covariance matrix of eq. (13) with $q_1 = 1 - 2x$ and where the components of \vec{q}_0 are considered as independent variables.

⁶ Here and below this 8-dimensional integration is to be understood as being performed with a uniform measure in the 5-dimensional subspace V_x , i.e. $\int_{V_x} d\mathbf{a} \equiv \int_{[0,1]^8} d\mathbf{a} \delta(a_4 + a_5 + a_6 + a_7 - x) \delta(a_1 + a_2 + a_5 + a_6 - x) \delta\left(\sum_{i=0}^7 a_i - 1\right)$, where δ is a Dirac delta, cf. eq. (16).

- $H_8(\vec{q}_0, \eta, x)$ is defined as the Shannon entropy of a probability mass function with masses corresponding to the components of the following vector:

$$\begin{pmatrix} \frac{1}{4}(q_{02} + q_{03} + 2 - 4x) + \eta \\ \frac{1}{4}(q_{01} - q_{02} + 2x) - \eta \\ \frac{1}{4}(-q_{03} + q_{04} + 2x) - \eta \\ \frac{1}{4}(2 - q_{01} - q_{04} - 4x) + \eta \\ \frac{1}{4}(q_{01} - q_{03} + 2x) - \eta \\ \eta \\ \frac{1}{4}(-q_{01} + q_{02} + q_{03} - q_{04}) + \eta \\ \frac{1}{4}(-q_{02} + q_{04} + 2x) - \eta \end{pmatrix}; \quad (20)$$

- \tilde{V}_x is the new domain of integration specified by the inequalities

$$\begin{cases} \frac{1}{4}(q_{01} - q_{02} + 2x - 4) \leq \eta \leq \frac{1}{4}(q_{01} - q_{02} + 2x) \\ \frac{1}{4}(-q_{03} + q_{04} + 2x - 4) \leq \eta \leq \frac{1}{4}(-q_{03} + q_{04} + 2x) \\ \frac{1}{4}(q_{01} + q_{04} + 4x - 2) \leq \eta \leq \frac{1}{4}(q_{01} + q_{04} + 4x + 2) \\ \frac{1}{4}(q_{01} - q_{03} + 2x - 4) \leq \eta \leq \frac{1}{4}(q_{01} - q_{03} + 2x) \\ 0 \leq \eta \leq 1 \\ \frac{1}{4}(q_{01} - q_{02} - q_{03} + q_{04}) \leq \eta \\ \frac{1}{4}(-q_{02} + q_{04} + 2x - 4) \leq \eta \leq \frac{1}{4}(-q_{02} + q_{04} + 2x) \\ \frac{1}{4}(-q_{02} - q_{03} + 4x - 2) \leq \eta \end{cases}, \quad (21)$$

some of which are already contained in eq. (20).

Proposition 1. For each K, x , define:

$$\Phi_{x,K,\alpha}(\vec{q}_0, \eta) = H_8(\vec{q}_0, \eta, x) - \ln 2 - 2H_2(x) + \alpha \ln f_2(\vec{q}_0, x, K) - 2\alpha \ln f_1(x, K). \quad (22)$$

and let $(\vec{q}_0^M, \eta^M) \in \tilde{V}_x$ be the global maximum of $\Phi_{x,K,\alpha}$ restricted to \tilde{V}_x . Then there exists a x, K -dependent constant $C > 0$ such that, for N sufficiently large,

$$\frac{\mathbb{E} [\mathcal{Z}_{y=2}(x, K, \xi)]^2}{\mathbb{E} [\mathcal{Z}_{y=2}^2(x, K, \xi)]} \geq C \exp \left(-N \Phi_{x,K,\alpha}(\vec{q}_0^M, \eta^M) \right). \quad (23)$$

Proof. Applying Laplace method to the integral in eq. (19), for some constant C_1 and for N large enough we obtain

$$\mathbb{E} [\mathcal{Z}_{y=2}^2(x, K, \xi)] \leq C_1 N^{-1} e^{N[\ln 2 + H_8(\vec{q}_0^M, \eta, x) + \alpha \ln f_2(\vec{q}_0^M, x, K)]}, \quad (24)$$

where the factor $N^{-1} = N^{\frac{3}{2} - \frac{5}{2}}$ stems from the Gaussian fluctuations around the 5-dimensional saddle point. For the first moment instead, a simple application of Stirling formula to eq. (5) leads, for some constant c_1 and N large enough, to

$$\mathbb{E} [\mathcal{Z}_{y=2}(x, K, \xi)]^2 \geq c_1 N^{-1} e^{2N[\ln 2 + H_2(x) + \alpha \ln f_1(x, K)]}. \quad (25)$$

Combining the two expressions, the proposition follows. \square

Given that $\Phi_{x,K,\alpha}(\vec{q}_0^M, \eta^M) \geq 0$, the second moment method gives a useful bound just when $\Phi_{x,K,\alpha}(\vec{q}_0^M, \eta^M) = 0$. If instead $\Phi_{x,K,\alpha}(\vec{q}_0^M, \eta^M) > 0$, the probability is bounded above zero (included) and the bound is non-informative.

For a particular point $(\vec{q}_0^*, \eta^*) \in \tilde{V}_x$, which can be interpreted intuitively as capturing the situation where the two pairs of solutions are uncorrelated, we have that $\Phi_{x,K,\alpha}(\vec{q}_0^*, \eta^*) = 0$ for all values of α . This point (\vec{q}_0^*, η^*) is specified by the following equations,

$$q_{01}^* = 0, q_{02}^* = 0, q_{03}^* = 0, q_{04}^* = 0, \eta^* = \frac{x^2}{2}. \quad (26)$$

In that case, we have the following properties:

- $H_8(\vec{q}_0^*, \eta^*, x) = \ln 2 + 2H_2(x)$,
- $f_2(\vec{q}_0^*, x, K) = f_1(x, K)^2$.

Therefore, α_{LB} is the largest value of α such that (\vec{q}_0^*, η^*) is a global maximum, i.e. such that there exists no $(\vec{q}_0, \eta) \in \tilde{V}_x$ with $\Phi_{x,K,\alpha}(\vec{q}_0, \eta) > 0$. In particular, for $\alpha = 0$ the second moment bound holds (proof in Appendix B 3):

$$\Phi_{x,K,\alpha=0}(\vec{q}_0, \eta) = H_8(\vec{q}_0, \eta, x) - \ln 2 - 2H_2(x) \leq 0 \quad \forall (\vec{q}_0, \eta) \in \tilde{V}_x. \quad (27)$$

Now, let us split \tilde{V}_x in the following way:

$$\tilde{V}_x^+ := \{(\vec{q}_0, \eta) \in \tilde{V}_x \mid f_2(\vec{q}_0, x, K) > f_1^2(x, K)\} \quad \text{and} \quad \tilde{V}_x^- := \{(\vec{q}_0, \eta) \in \tilde{V}_x \mid f_2(\vec{q}_0, x, K) \leq f_1^2(x, K)\}.$$

It follows that for all $(\vec{q}_0, \eta) \in \tilde{V}_x^-$ and $\alpha > 0$ we have

$$\Phi_{x,K,\alpha}(\vec{q}_0, \eta) \leq \Phi_{x,K,\alpha=0}(\vec{q}_0, \eta) \leq 0.$$

As already discussed, α_{LB} is the largest value of α such that

$$\max_{(\vec{q}_0, \eta) \in \tilde{V}_x} \Phi_{x,K,\alpha}(\vec{q}_0, \eta) = 0.$$

From the previous observation

$$\max_{(\vec{q}_0, \eta) \in \tilde{V}_x} \Phi_{x,K,\alpha}(\vec{q}_0, \eta) = \sup_{(\vec{q}_0, \eta) \in \tilde{V}_x^+} \Phi_{x,K,\alpha}(\vec{q}_0, \eta),$$

and therefore α_{LB} is the largest value of α such that

$$\sup_{(\vec{q}_0, \eta) \in \tilde{V}_x^+} \Phi_{x,K,\alpha}(\vec{q}_0, \eta) = 0.$$

Then, α_{LB} is the largest value of α such that there exists no $(\vec{q}_0, \eta) \in \tilde{V}_x^+$ with $\Phi_{x,K,\alpha}(\vec{q}_0, \eta) > 0$, which is true if and only if

$$H_8(\vec{q}_0, \eta, x) - \ln 2 - 2H_2(x) + \alpha \ln f_2(\vec{q}_0, x, K) - 2\alpha \ln f_1(x, K) \leq 0 \quad \forall (\vec{q}_0, \eta) \in \tilde{V}_x^+, \quad \forall \alpha \leq \alpha_{LB}. \quad (28)$$

Therefore, eq. (28) implies that for $\alpha \leq \alpha_{LB}$ the following condition must hold as well:

$$\alpha \leq \frac{\ln 2 + 2H_2(x) - H_8(\vec{q}_0, \eta, x)}{\ln f_2(\vec{q}_0, x, K) - 2 \ln f_1(x, K)} \quad \forall (\vec{q}_0, \eta) \in \tilde{V}_x^+. \quad (29)$$

We obtain the following result:

Lower Bound. For each K and $0 < x < 1$, and for all α such that

$$\alpha < \alpha_{LB}(x, K) \equiv \inf_{(\vec{q}_0, \eta) \in \tilde{V}_x^+} \frac{\ln 2 + 2H_2(x) - H_8(\vec{q}_0, \eta, x)}{\ln f_2(\vec{q}_0, x, K) - 2 \ln f_1(x, K)} \quad (30)$$

we have that there is a positive probability of finding SAT- x -pairs of solutions, namely

$$\liminf_{N \rightarrow \infty} \mathbb{P} [\mathcal{Z}_{y=2}(x, K, \xi) > 0] > 0. \quad (31)$$

The optimization can be simplified further by slicing the set \tilde{V}_x^+ in the two “directions” \vec{q}_0 and η . We define a \vec{q}_0 -slice as $(\tilde{V}_x^+)_{\vec{q}_0} := \{\eta \mid (\vec{q}_0, \eta) \in \tilde{V}_x^+\}$ and the natural projection of the set \tilde{V}_x^+ on the \vec{q}_0 -subspace as $\pi_{\vec{q}_0}(\tilde{V}_x^+) = \{\vec{q}_0 \mid \exists \eta \text{ s.t. } (\vec{q}_0, \eta) \in \tilde{V}_x^+\}$. With this notation, eq. (30) becomes:

$$\alpha_{LB}(x, K) = \inf_{\vec{q}_0 \in \pi_{\vec{q}_0}(\tilde{V}_x^+)} \frac{\ln 2 + 2H_2(x) - \sup_{\eta \in (\tilde{V}_x^+)_{\vec{q}_0}} H_8(\vec{q}_0, \eta, x)}{\ln f_2(\vec{q}_0, x, K) - 2 \ln f_1(x, K)}. \quad (32)$$

The optimization in η is easy because the function $H_8(\vec{q}_0, \eta)$ is concave in η for each \vec{q}_0 . This is not necessarily true for the optimization in \vec{q}_0 . In fact, it is crucial that we find the global optimum of the objective function because this gives the correct value for the lower bound. To this purpose we have devised two computational strategies. First we evaluated the objective function on a 4-dimensional grid with increasing number of points. Then we have also implemented a simple gradient descent starting from the points of the grid. The different strategies are discussed in Appendix B 4.

The bounds that we obtain in fig. 2 are symmetric around the value $x = 0.5$ and there are two critical values $x_c, x'_c \in [0, 0.5]$ (plus the symmetric ones, $1 - x_c$ and $1 - x'_c$) that delimit regions characterized by two different phases. For values of x such that $x_c \leq x \leq x'_c$ or $1 - x'_c \leq x \leq 1 - x_c$ all four entries of \vec{q}_0 take the same value. We use the subscript S to denote this kind of solution. Instead for $x \leq x_c$, $x \geq 1 - x_c$ and $x'_c \leq x \leq 1 - x'_c$, this symmetry is broken and the optimum is achieved on a different point that we call Symmetry Broken (SB) solution. This point has the property that the two pairs of binary vectors of solutions $(\mathbf{w}_1, \mathbf{w}_2)$ and $(\tilde{\mathbf{w}}_1, \tilde{\mathbf{w}}_2)$ coincide, as can be seen from the structure of the covariance matrix. We report below the covariance structure of the two solutions, where we adopted the convention $q_1 := 1 - 2x$. The symmetric covariance matrix is the following:

$$\Sigma_S = \begin{pmatrix} 1 & q_1 & q_0 & q_0 \\ q_1 & 1 & q_0 & q_0 \\ q_0 & q_0 & 1 & q_1 \\ q_0 & q_0 & q_1 & 1 \end{pmatrix}, \quad (33)$$

while the one corresponding to point SB is the following:

$$\Sigma_{SB} = \begin{pmatrix} 1 & q_1 & 1 & q_1 \\ q_1 & 1 & q_1 & 1 \\ 1 & q_1 & 1 & q_1 \\ q_1 & 1 & q_1 & 1 \end{pmatrix}. \quad (34)$$

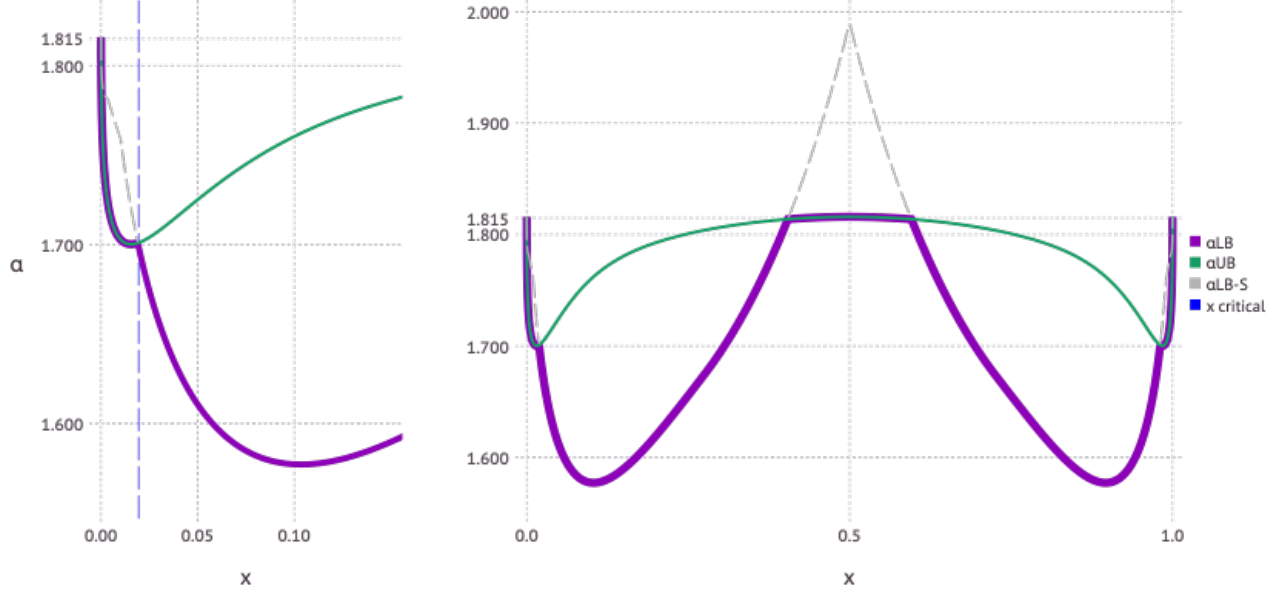


Figure 2. Lower and upper bounds for the RBP with $K = 1$. (Left) Lower and upper bounds on the whole range $x \in [0, 1]$. These bounds are symmetric around the vertical axis that passes by $x = 0.5$. In correspondence of the SB solution, the lower bound prediction from the S point (gray line) is larger than the upper bound and therefore patently wrong. This is what happens in the regions $x \leq x_c$, $x \geq 1 - x_c$ and $x'_c \leq x \leq 1 - x'_c$, where the two critical values $x_c \approx 0.195 \dots$ and $x'_c \approx 0.405 \dots$ are highlighted by the blue vertical lines on the left of the symmetry axis. In the regions $x_c \leq x \leq x'_c$ and $1 - x'_c \leq x \leq 1 - x_c$, there is a gap between the lower (purple line) and the upper bound (green line) where the S solution is indeed valid. (Right) Zoom of the figure on the left, in the region around x_c . Here, for $x \leq x_c$ the S solution fails. This is evident from the fact that the symmetric lower bound becomes bigger than the upper bound (gray line). In this region instead, the true lower bound perfectly matches the upper bound since the optimum of eq. (38) is in correspondence of the SB solution.

This is a degenerate covariance matrix, and in correspondence of the SB solution it follows from the previous equations that the lower bound and the upper bound coincide.

The physical meaning of what happens is qualitatively different for these two phases. Let us take $x < x_c$, where the bounds are tight, and let's start with low α and progressively increase it. In this regime the typical overlap between pairs of solutions is zero, i.e. the two pairs of solutions are independent and there is a positive probability of finding SAT- x -pairs since we are below α_{LB} . When we reach $\alpha = \alpha_{LB} = \alpha_{UB}$ there is a transition to a regime where w.h.p. there exists no pair of solutions to the problem. When this happens the point $(\tilde{q}_0^M, \eta^M) \in \tilde{V}_x$ that optimizes (22) is the SB point. For $x_c < x < x'_c$, the bounds are no longer tight and we can only identify a region between the two bounds where a SAT/UNSAT transition occurs. Again, for $x'_c < x \leq 0.5$ the bounds are tight. For $x > 0.5$ the behavior is symmetric to the one that we have just described.

IV. MULTIPLETS OF SOLUTIONS ($y > 2$)

In the previous section we were able to derive rigorous expressions for the upper bound $\alpha_{UB}(x)$, in eq. (9), and the lower bound $\alpha_{LB}(x)$, in eq. (32), obtained by first and second moment calculations, such that w.h.p. no pairs of solutions at distance x exist for load $\alpha > \alpha_{UB}(x)$ and at least one pair exists for $\alpha < \alpha_{LB}(x)$. It would be then natural to try to generalize the

derivation to sets of y solutions at pairwise distance x (multiplets) and in particular asses the existence of a small α regime where such sets can be found for any value of y and for small enough x . This result would rigorously confirm the existence of a dense region of solutions as derived in sec. II, which in turn has been non-rigorously advocated as a necessary condition for the existence of efficient learning algorithms [12].

Unfortunately, it is technically unfeasible to carry out the rigorous derivation for $y > 2$ as we have done above for the case $y = 2$. Therefore, in this section, after giving an rigorous expression for the first moment upper bound limited to the cases $y = 3$ and $y = 4$, we will derive compact expressions for the first and second moment bound using non-rigorous field theoretical calculations and a replica symmetric ansatz. We find that the non-rigorous results match the rigorous ones when available, although we expect the prediction to break down at large values of y due to replica symmetry breaking effects (see the discussion in the Introduction).

A. Rigorous first moment upper bounds

In the following we derive the rigorous expressions for the first moment bound in two additional cases: the existence of triplets and quadruplets of solutions at fixed pairwise distance x .

1. Triplets ($y = 3$)

Let us define the symbol \cong as equivalence up to sub-exponential terms as $N \rightarrow \infty$, that is for any two sequences $(a_N)_N$ and $(b_N)_N$ we write $a_N \cong b_N$ iff $\lim_{N \rightarrow \infty} \frac{\ln a_N}{\ln b_N} = 1$. The first moment of the triplets partition function has the following asymptotic expression:

$$\begin{aligned} \mathbb{E} [\mathcal{Z}_{y=3}(x, K, \xi)] &\cong 2^N \binom{N}{\frac{Nx}{2}, \frac{Nx}{2}, \frac{Nx}{2}} \mathbb{P}[v_1 \in I_K, v_2 \in I_K, v_3 \in I_K]^M \\ &\cong e^{N(\ln(2) + H_4(x) + \alpha \ln f_1^{y=3}(x, K))}, \end{aligned} \quad (35)$$

where $H_4(x) = -\frac{3}{2}x \ln(\frac{x}{2}) - (1 - \frac{3}{2}x) \ln(1 - \frac{3}{2}x)$ and we get the geometric condition $0 < x < \frac{2}{3}$, and $f_1^{y=3}(x, K)$ is the probability that a zero mean Gaussian random vector $\vec{v}_3 = (v_1, v_2, v_3)$, whose covariance matrix Σ_3 has ones on the diagonal and $1 - 2x$ off-diagonal, takes values in the box $[-K, K]^3$, that is

$$f_1^{y=3}(x, K) = \frac{1}{(2\pi)^{\frac{3}{2}} |\Sigma_3|^{1/2}} \int_{[-K, K]^3} dv_1 dv_2 dv_3 e^{-\vec{v}_3^T \Sigma_3^{-1} \vec{v}_3}. \quad (36)$$

An equivalent argument to the case $y = 2$ gives the following upper bound for the existence of clusters of three solutions:

$$\alpha_{UB}^{y=3}(x, K) = -\frac{\ln 2 + H_4(x)}{\ln f_1^{y=3}(x, K)}. \quad (37)$$

2. Quadruplets ($y = 4$)

For quadruplets of solutions, we have

$$\mathbb{E} [\mathcal{Z}_{y=4}(x, K, \xi)] \cong 2^N \sum_{\mathbf{a} \in V_{N,x}^{y=4} \cap \{0, 1/N, 2/N, \dots, 1\}^8} \frac{N!}{\prod_{i=0}^7 (Na_i)!} \left[f_1^{y=4}(x, K) \right]^M, \quad (38)$$

where:

- In complete analogy with the previous case $f_1^{y=4}(x, K)$ is the probability that a zero mean Gaussian random vector $\vec{v}_4 = (v_1, v_2, v_3, v_4)$, whose covariance matrix Σ_4 has ones on the diagonal and $1 - 2x$ off-diagonal, takes values in the box $[-K, K]^4$, that is

$$f_1^{y=4}(x, K) = \frac{1}{(2\pi)^2 |\Sigma_4|^{1/2}} \int_{[-K, K]^4} d\vec{v}_4 e^{-\vec{v}_4^T \Sigma_4^{-1} \vec{v}_4}. \quad (39)$$

- The summation is restricted to the set $V_{N,x}^{y=4} \subseteq [0, 1]^8$, specified by:

$$\begin{cases} \lfloor N(a_4 + a_5 + a_6 + a_7) \rfloor = \lfloor Nx \rfloor \\ \lfloor N(a_1 + a_2 + a_5 + a_6) \rfloor = \lfloor Nx \rfloor \\ \lfloor N(a_2 + a_3 + a_6 + a_7) \rfloor = \lfloor Nx \rfloor \\ \lfloor N(a_1 + a_3 + a_5 + a_7) \rfloor = \lfloor Nx \rfloor \\ \lfloor N(a_2 + a_3 + a_4 + a_5) \rfloor = \lfloor Nx \rfloor \\ \lfloor N(a_1 + a_3 + a_4 + a_6) \rfloor = \lfloor Nx \rfloor \\ \sum_{i=0}^7 a_i = 1 \end{cases} \quad (40)$$

In the limit $N \rightarrow \infty$, due to the 7 constraints in eq. (40), the summation over elements in the box $[0, 1]^8$ in eq. (38) can be replaced by an integral over the interval

$$\mathcal{B}_x \equiv \left[0, \min \left\{ \frac{x}{2}, 1 - \frac{3}{2}x \right\} \right] \quad \text{for } x < \frac{2}{3}, \quad (41)$$

while for $x > \frac{2}{3}$ the constraints admit no solutions and $\mathbb{E} [\mathcal{Z}_{y=4}(x, K, \xi)] \cong 0$.

Therefore, for $x < \frac{2}{3}$, we can write

$$\begin{aligned} \mathbb{E} [\mathcal{Z}_{y=4}(x, K, \xi)] &\cong 2^N \int_{\mathcal{B}_x} db \binom{N}{N(1-b-\frac{3}{2}x), Nb, Nb, N(\frac{x}{2}-b), Nb, N(\frac{x}{2}-b), N(\frac{x}{2}-b), Nb} f_1^{y=4}(x, K) \\ &\cong \int_{\mathcal{B}_x} db e^{N(\ln 2 + H_8(x, b) + \ln f_1^{y=4}(x, K))} \\ &\cong e^{N(\ln 2 + H_8(x, b^*(x)) + \ln f_1^{y=4}(x))}, \end{aligned}$$

where in the last line we estimated the integral with its saddle point contribution at $b^*(x) = \arg\max_{b \in \mathcal{B}_x} H_8(x, b)$. The function $H_8(x, b)$ is the Shannon entropy of an eight-states discrete probability distribution with masses given by the components of the vector $(1 - b - 3/2 x, b, b, x/2 - b, b, x/2 - b, x/2 - b, b)$. It follows that the first moment upper bound to the storage capacity for quadruplets of solutions at a fixed distance x is given by

$$\alpha_{UB}^{y=4}(x, K) = -\frac{\ln 2 + H_8(x, b^*(x))}{\ln f_1^{y=4}(x, K)}.$$

The numerical evaluation of the two upper bounds, $y = 3$ and $y = 4$, can be found in fig. 3 along with the predictions for the upper bound from non-rigorous calculations for larger y 's.

B. Upper bounds under symmetric assumption for saddle point

Since a rigorous expression for the upper bound $\alpha_{UB}^y(x, K)$ for $y > 4$ is hard to derive, due to highly non-trivial combinatorial factors, we resort to non-rigorous field theoretical techniques and replica symmetric ansatz to obtain an expression that we believe to be exact for low values of y but is likely slightly incorrect for very large y due to replica symmetry breaking effects. The generic computation of the n -th moment of the partition function, $\mathbb{E}[\mathcal{Z}_y^n]$, is shown in Appendix C. Here we present the final result for the first moment bound, i.e. the case $n = 1$.

In what follows, we denote with SP the saddle point operation, and we use the overlap between solutions $q_1 \equiv 1 - 2x$ as our control parameter instead of the distance x to match the usual notation of replica theory calculations. Up to subleading terms in N as $N \rightarrow \infty$ we have:

$$\mathbb{E}[\mathcal{Z}_y(q_1, K, \xi)] \cong e^{N \left(\text{SP}_{\hat{q}_1} \left\{ G_{IS}^{n=1,y}(q_1, \hat{q}_1) \right\} + \alpha G_E^{n=1,y,K}(q_1) \right)},$$

where

$$G_{IS}^{n=1,y}(q_1, \hat{q}_1) = -q_1 \hat{q}_1 \frac{y(y-1)}{2} - \frac{\hat{q}_1 y}{2} + \ln \int Dt \left(2 \cosh(t \sqrt{\hat{q}_1}) \right)^y$$

$$G_E^{n=1,y,K}(q_1) = \ln \int Dz \left[\sum_{s=\pm 1} s H \left(\frac{-sK}{\sqrt{1-q_1}} + \frac{\sqrt{q_1} z}{\sqrt{1-q_1}} \right) \right]^y$$

where we have used the shorthand notation for standard Gaussian integrals $Dz \equiv dz \frac{e^{-\frac{z^2}{2}}}{\sqrt{2\pi}}$, and the definition $H(x) = \int_x^\infty Dz = \frac{1}{2} \text{erfc} \left(\frac{x}{\sqrt{2}} \right)$.

The first moment bound therefore implies that in the limit $N \rightarrow \infty$ there are no SAT- x multiplets of y solutions if

$$\text{SP}_{\hat{q}_1} \left\{ G_{IS}^{n=1,y}(q_1, \hat{q}_1) \right\} + \alpha G_E^{n=1,y,K}(q_1) < 0. \quad (42)$$

This leads to an estimation $\alpha_{UB,S}^y$ given by the symmetric saddle point of the true upper bound α_{UB}^y that takes the form

$$\alpha_{UB,S}^y(q_1, K) \equiv - \frac{\text{SP}_{\hat{q}_1} \left\{ G_{IS}^{n=1,y}(q_1, \hat{q}_1) \right\}}{G_E^{n=1,y,K}(q_1)}. \quad (43)$$

These expressions are derived under a symmetric ansatz (i.e. we restrict the search for the saddle point to a particular subset of the region of integration) and thus are not rigorous; yet the results in the cases $y = 2, 3, 4$ agree with the rigorous ones. The corresponding curves are shown in fig. 3. Notice that for some values and y and x , the second moment upper bound is larger than the critical value for the single (and less constrained) system, $\alpha_{UB}^y(x) > \alpha_c$. Since the replicated system critical value, if exist, is such that $\alpha_c^y(x) \leq \alpha_c$, in that parameter region the upper bound is not tight.

As one can see, the curves intersect in a nontrivial way. Let's take for example the curves for $y = 2$ and $y = 3$. If the bounds were tight for all values of x , the curve at $y = 3$ should always stay below the curve for $y = 2$. This follows directly from the fact that if we have no way of accommodating pairs of solutions then we do not have a way to accommodate triplets solutions either. Instead, the fact that the curves intersect means that for values of x smaller than the intersection point the bounds stop being tight. This straightforward argument, generalized to higher values of y , therefore we can define a tighter upper bound, that we call $\tilde{\alpha}_{UB}^y(x, K)$, for the existence of sets of y constrained solutions:

$$\tilde{\alpha}_{UB}^y(x, K) = \min \left\{ \alpha_{UB}^{y'}(x, K) : y' \in \mathbb{N}, 2 \leq y' \leq y \right\}. \quad (44)$$

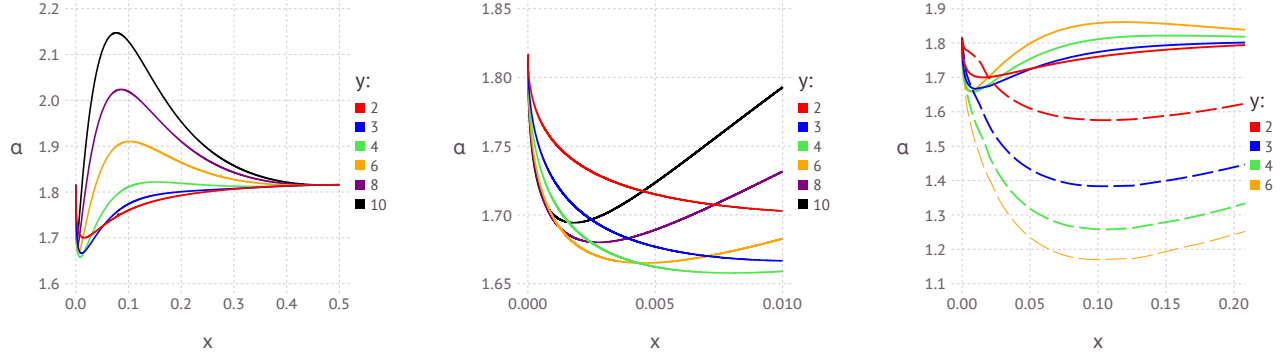


Figure 3. (Left) Upper bound $\alpha^y_{UB}(x, K=1)$ to the SAT/UNSAT threshold for the RBP problem with y replicas constrained at pairwise distance x . Curves are given by rigorous derivation ($y = 2, 3, 4$) or by non-rigorous field theoretical calculations (43) ($y > 4$). (Center) Zoom of the figure on the left. Close to $x = 0$ the curves corresponding to different y intersect. (Right) The upper bounds (solid lines) are compared to the S point predictions (52) for the lower bounds (dashed lines).

C. Lower bounds under symmetric assumption for the saddle point

We compute the partition function moments needed for the lower bounds in Appendix C. The final result of the replica calculation is given by

$$\begin{aligned} \mathbb{E} [\mathcal{Z}_y^2(q_1, K, \xi)] &\cong \exp \left(N \cdot \text{SP}_{q_0 \hat{q}_0 \hat{q}_1} \left\{ -\hat{q}_1 y - y [y q_0 \hat{q}_0 + (y-1) q_1 \hat{q}_1] \right. \right. \\ &\quad \left. \left. + \ln \int Dz \left[\int Dt \left(2 \cosh \left(\sqrt{\hat{q}_0} z + \sqrt{\hat{q}_1 - \hat{q}_0} t \right) \right)^y \right]^2 \right. \right. \\ &\quad \left. \left. + \alpha \ln \int Dz \left[\int Dt \left[\sum_{s=\pm 1} s H \left(\frac{-s K}{\sqrt{1-q_1}} + \frac{\sqrt{q_0} z + \sqrt{q_1 - q_0} t}{\sqrt{1-q_1}} \right) \right]^y \right]^2 \right. \right. \end{aligned} \quad (45)$$

$$= \exp \left(N \cdot \text{SP}_{q_0 \hat{q}_0 \hat{q}_1} \left\{ G_I^{n=2,y}(q_0, \hat{q}_0, q_1, \hat{q}_1) + G_S^{n=2,y}(\hat{q}_0, \hat{q}_1) + \alpha G_E^{n=2,y,K}(q_0, q_1) \right\} \right), \quad (46)$$

where

$$G_I^{n=2,y}(q_0, \hat{q}_0, q_1, \hat{q}_1) = -\hat{q}_1 y - y [y q_0 \hat{q}_0 + (y-1) q_1 \hat{q}_1] \quad (47)$$

$$G_S^{n=2,y}(\hat{q}_0, \hat{q}_1) = \ln \int Dz \left[\int Dt \left(2 \cosh \left(\sqrt{\hat{q}_0} z + \sqrt{\hat{q}_1 - \hat{q}_0} t \right) \right)^y \right]^2 \quad (48)$$

$$G_E^{n=2,y,K}(q_0, q_1) = \ln \int Dz \left[\int Dt \left[\sum_{s=\pm 1} s H \left(\frac{-s K}{\sqrt{1-q_1}} + \frac{\sqrt{q_0} z + \sqrt{q_1 - q_0} t}{\sqrt{1-q_1}} \right) \right]^y \right]^2. \quad (49)$$

Performing the saddle points over the variables \hat{q}_0 and \hat{q}_1 , these expressions reduce to

$$\mathbb{E} [\mathcal{Z}_y^2(q_1, K, \xi)] \simeq e^{N(\max_{q_0} \{G_{IS}^{\text{opt}, n=2, y}(q_0, q_1) + \alpha G_E^{n=2, y, K}(q_0, q_1)\})}, \quad (50)$$

where

$$G_{IS}^{\text{opt}, n=2, y}(q_0, q_1) = \text{SP}_{\hat{q}_0 \hat{q}_1} \left\{ G_I^{n=2, y}(q_0, \hat{q}_0, q_1, \hat{q}_1) + G_S^{n=2, y}(\hat{q}_0, \hat{q}_1) \right\}. \quad (51)$$

For fixed α , if the optimum in eq. (50) is at $q_0 = 0$ we have $\mathbb{E} [\mathcal{Z}_y^2(q_1, K, \xi)] \cong \mathbb{E} [\mathcal{Z}_y(q_1, K, \xi)]^2$ and from the second moment inequality, eq. (10), we have that there is positive probability of finding multiplets of y solutions at distance $x = \frac{1}{2}(1 - q_1)$. This in turn implies that the lower bound is valid for all α 's such that $\text{argmax}_{q_0} \{G_{IS}^{\text{opt}, n=2, y}(q_0, q_1) + \alpha G_E^{n=2, y, K}(q_0, q_1)\} = 0$. In particular the symmetric saddle point prediction for the lower bound is given by

$$\alpha_{LB, S}^y(q_1) = \sup \left\{ \alpha \geq 0 \left| \text{argmax}_{q_0} \{G_{IS}^{\text{opt}, n=2, y}(q_0, q_1) + \alpha G_E^{n=2, y, K}(q_0, q_1)\} = 0 \right. \right\}. \quad (52)$$

The results for $y = 2, 3, 4, 5$ are summarized in fig. 3 on the right. In fig. 4 we plot an enlargement of the small-distance region around $x = 0$, corresponding to $q_1 = 1$. We find that in all cases there is an inconsistency region $[0, x_c(y)]$ in which the symmetric lower and upper bounds switch roles, similarly to what happened in the case of $y = 2$ (see fig. 2). The true lower bound cannot thus be symmetric in this region: the configuration in which the two SAT- x multiplets of y solutions are collapsed on a single multiplet always gives a better saddle point, resulting in a lower bound equal to the upper bound. We thus conjecture that for $x < x_c(y)$ the bounds are tight, like in the $y = 2$ case. The symmetry of lower and upper bounds with respect to x on the interval $[0, 1]$ (or the corresponding symmetry for q_1) which holds for $y = 2$ does not apply to general y . In our numerical exploration presented in fig. 3, we focused on the region of small x . We also notice that the lower bounds for increasing y 's decrease monotonically, and in the limit $y \rightarrow \infty$ the limiting curve seem to exhibit a vertical asymptote for $x = 0$. Furthermore, the intersection point $x_c(y)$ seem to decrease monotonically with y and to approach zero. It is also worth noting that, for all the y that we tested, we found that in the region $[0, x_c(y)]$ we have $\tilde{\alpha}_{UB}^y = \alpha_{UB}^y$, which is consistent with the conjecture that the bounds are tight in this region.

V. CONCLUSIONS

We have presented an investigation of the geometry of the solutions space for the binary symmetric perceptron model storing random patterns. According to the non-rigorous analysis conducted with the replica method, this model exhibits the same qualitative phenomenology as the more standard non-symmetric counterpart. In particular, we focused on signatures for the presence of rare dense regions of solutions, which are of particular interest since according to previous studies they appear to be crucially connected to the existence of efficient learning algorithms [12?]. The analogous structures for continuous models (of the kind used for deep learning applications) are wide flat minima, which have also been related to training efficiency and generalization capabilities [?].

Compared to standard models, the symmetry in the model used for this paper simplifies the analytical treatment, as was first shown in ref. [17]. Thanks to this, we have been able to show rigorously (up to a numerical optimization step) that in the large N limit there exist an exponential number of pairs of solution at arbitrary $O(N)$ Hamming distance. A further analysis led us to conjecture that this scenario extends to multiplets of more than 2 solutions at fixed distance. These results are highly non-trivial, and consistent with the replica analysis; a complete and rigorous confirmation will presumably require different tools or alternative approaches however, and thus remains as an open problem. Besides this, several other important problems

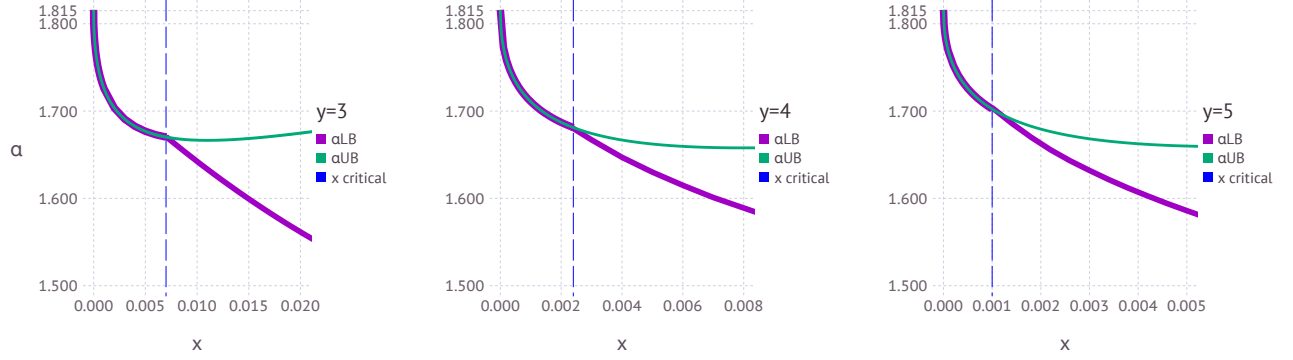


Figure 4. Lower and upper bounds for the RBP with $K = 1$ and for different values of $y = 3, 4, 5$, in the region of small x . Like in the case of $y = 2$, for x larger than the critical value $x_c(y)$ (blue vertical line) there is a gap between the symmetric lower bound (purple line) and the upper bound (green line). This gap closes in correspondence of the *SB* solution for $x \leq x_c(y)$ and the two bounds coincide.

related to the dense regions, with potentially far-fetching practical and theoretical implications, remain open: in particular, obtaining a detailed description of their geometry, and a complete characterization of their accessibility by efficient algorithms.

-
- [1] Elizabeth Gardner and Bernard Derrida. Optimal storage properties of neural network models. *Journal of Physics A: Mathematical and General*, 21(1):271–284, jan 1988. doi:[10.1088/0305-4470/21/1/031](https://doi.org/10.1088/0305-4470/21/1/031).
 - [2] Timothy L. H. Watkin, Albrecht Rau, and Michael Biehl. The statistical mechanics of learning a rule. *Reviews of Modern Physics*, 65:499–556, Apr 1993. doi:[10.1103/RevModPhys.65.499](https://doi.org/10.1103/RevModPhys.65.499).
 - [3] Hyunjun Sebastian Seung, Haim Sompolinsky, and Naftali Tishby. Statistical mechanics of learning from examples. *Physical Review A*, 45:6056–6091, Apr 1992. doi:[10.1103/PhysRevA.45.6056](https://doi.org/10.1103/PhysRevA.45.6056).
 - [4] Andreas Engel and Christian Van den Broeck. *Statistical mechanics of learning*. Cambridge University Press, 2001. doi:[10.1017/CB09781139164542](https://doi.org/10.1017/CB09781139164542).
 - [5] Werner Krauth and Marc Mézard. Storage capacity of memory networks with binary couplings. *Journal de Physique*, 50(20):3057–3066, 1989. doi:[10.1051/jphys:0198900500200305700](https://doi.org/10.1051/jphys:0198900500200305700).
 - [6] Haiping Huang, K. Y. Michael Wong, and Yoshiyuki Kabashima. Entropy landscape of solutions in the binary perceptron problem. *Journal of Physics A: Mathematical and Theoretical*, 46(37):375002, aug 2013. doi:[10.1088/1751-8113/46/37/375002](https://doi.org/10.1088/1751-8113/46/37/375002).
 - [7] Haiping Huang and Yoshiyuki Kabashima. Origin of the computational hardness for learning with binary synapses. *Physical Review E*, 90(5):052813, 2014. doi:<https://doi.org/10.1103/PhysRevE.90.052813>.
 - [8] Alfredo Braunstein and Riccardo Zecchina. Learning by message passing in networks of discrete synapses. *Physical Review Letters*, 96:030201, Jan 2006. doi:[10.1103/PhysRevLett.96.030201](https://doi.org/10.1103/PhysRevLett.96.030201).
 - [9] Carlo Baldassi, Alfredo Braunstein, Nicolas Brunel, and Riccardo Zecchina. Efficient supervised learning in networks with binary synapses. *Proceedings of the National Academy of Sciences of the United States of America*, 104(26):11079–1084, 2007. doi:[10.1073/pnas.0700324104](https://doi.org/10.1073/pnas.0700324104).
 - [10] Carlo Baldassi. Generalization learning in a perceptron with binary synapses. *Journal of Statistical Physics*, 136(5):902–916, 2009. doi:[10.1007/s10955-009-9822-1](https://doi.org/10.1007/s10955-009-9822-1).
 - [11] Carlo Baldassi and Alfredo Braunstein. A max-sum algorithm for training discrete neural networks. *Journal of Statistical Mechanics: Theory and Experiment*, 2015(8):P08008, 2015. doi:[10.1088/1742-5468/2015/08/P08008](https://doi.org/10.1088/1742-5468/2015/08/P08008).
 - [12] Carlo Baldassi, Alessandro Ingrosso, Carlo Lucibello, Luca Saglietti, and Riccardo Zecchina. Subdominant dense clusters allow for simple learning and high computational performance in neural networks with discrete synapses. *Phys. Rev. Lett.*, 115:128101, Sep

2015. doi:10.1103/PhysRevLett.115.128101.
- [13] Carlo Baldassi, Alessandro Ingrosso, Carlo Lucibello, Luca Saglietti, and Riccardo Zecchina. Local entropy as a measure for sampling solutions in constraint satisfaction problems. *Journal of Statistical Mechanics: Theory and Experiment*, 2016(2):P023301, February 2016. doi:10.1088/1742-5468/2016/02/023301.
- [14] Carlo Baldassi, Fabrizio Pittorino, and Riccardo Zecchina. Shaping the learning landscape in neural networks around wide flat minima. *arXiv preprint arXiv:1905.07833*, 2019. URL: <https://arxiv.org/abs/1905.07833>.
- [15] Carlo Baldassi, Enrico M Malatesta, and Riccardo Zecchina. Properties of the geometry of solutions and capacity of multilayer neural networks with rectified linear unit activations. *Physical Review Letters*, 123(17):170602, 2019. doi:10.1103/PhysRevLett.123.170602.
- [16] Jian Ding and Nike Sun. Capacity lower bound for the ising perceptron. In *Proceedings of the 51st Annual ACM SIGACT Symposium on Theory of Computing*, pages 816–827. ACM, 2019. doi:10.1145/3313276.3316383.
- [17] Benjamin Aubin, Will Perkins, and Lenka Zdeborová. Storage capacity in symmetric binary perceptrons. *Journal of Physics A: Mathematical and Theoretical*, 52(29):294003, jun 2019. doi:10.1088/1751-8121/ab227a.
- [18] Marc Mézard, Thierry Mora, and Riccardo Zecchina. Clustering of solutions in the random satisfiability problem. *Physical Review Letters*, 94:197205, May 2005. doi:10.1103/PhysRevLett.94.197205.
- [19] Hervé Daudé, Marc Mézard, Thierry Mora, and Riccardo Zecchina. Pairs of sat-assignments in random boolean formulae. *Theoretical Computer Science*, 393(1):260–279, 2008. doi:10.1016/j.tcs.2008.01.005.

Appendix A: $y \rightarrow \infty$ limit

In this Section we derive the large y limit of the entropy

$$\phi_y(x, K, \alpha) = \lim_{N \rightarrow \infty} \frac{1}{yN} \mathbb{E}_{\xi} \ln \mathcal{Z}_y(x, K, \xi)$$

within RS assumptions. For convenience of notation we will use the overlap $q_1 = 1 - 2x$ instead of x . As explained in ref. [?], the computation of $\phi_y(x)$ is formally equivalent to that of a single replica in the 1RSB ansatz with Parisi parameter y , except for the fact that q_1 is fixed externally instead of being optimized as usual. We obtain the following entropy for the Random Binary Perceptron (RBP) with y real replicas:

$$\phi_y(x, K, \alpha) = \underset{q_0 \ q_1}{\text{SP}} \left\{ -\frac{\hat{q}_1}{2} (1 - q_1) + \frac{y}{2} (q_0 \hat{q}_0 - q_1 \hat{q}_1) + \frac{1}{y} \int D z_0 \ln \int D z_1 \left[2 \cosh \left(\sqrt{\hat{q}_0} z_0 + \sqrt{\hat{q}_1 - \hat{q}_0} z_1 \right) \right]^y + \right. \quad (\text{A1})$$

$$\left. + \frac{\alpha}{y} \int D z_0 \ln \int D z_1 \left[\sum_{s=\pm 1} s H \left(\frac{-s K}{\sqrt{1 - q_1}} + \frac{\sqrt{\hat{q}_0} z_0 + \sqrt{\hat{q}_1 - \hat{q}_0} z_1}{\sqrt{1 - q_1}} \right) \right]^y \right\}. \quad (\text{A2})$$

We want to take the limit $y \rightarrow \infty$ in the previous expression. By looking at the entropic and energetic parts we derive the appropriate scalings

$$\hat{q}_0 = \hat{q}_1 - \frac{\delta \hat{q}}{y}, \quad q_0 = q_1 - \frac{\delta q}{y}, \quad (\text{A3})$$

and the previous equation becomes

$$\phi_{y=\infty}(q_1, K, \alpha) = \underset{\delta q \ \delta \hat{q}}{\text{SP}} \left\{ -\frac{\hat{q}_1}{2} (1 - q_1) - \frac{1}{2} (\delta q \hat{q}_1 + \delta \hat{q} q_1) + \int D z_0 A^*(z_0) + \alpha \int D z_0 B^*(z_0) \right\}, \quad (\text{A4})$$

where

$$A^*(z_0) = \ln 2 - \min_{z_1} \left\{ \frac{z_1^2}{2} - \ln \cosh \left(\sqrt{q_1} z_0 + \sqrt{\delta q} z_1 \right) \right\}, \quad (\text{A5})$$

$$B^*(z_0) = - \min_{z_1} \left\{ \frac{z_1^2}{2} - \ln \left[\sum_{s=\pm 1} s H \left(\frac{-s K}{\sqrt{1-q_1}} + \frac{\sqrt{q_1} z_0 + \sqrt{\delta q} z_1}{\sqrt{1-q_1}} \right) \right] \right\}. \quad (\text{A6})$$

The results are shown in fig. 1. The behavior of $\phi_{y=\infty}(q_1)$ close to $q_1 = 1$, where it approaches the maximum volume curve, reveals the existence of a dense cluster of solutions. Furthermore, the maximum volume curve coincides with the curve for $\alpha = 0$, which means that there are no constraints to impose and the function $\phi_{y=\infty}(q_1, K, 0) = H_2((1 + \sqrt{q_1})/2)$. We expect the value obtained within the RS ansatz for $\phi_{y=\infty}(q_1, K, \alpha)$ to not be the correct one, at least for α above some critical value where spin glass instabilities arise. In fact $\phi_{y=\infty}(q_1, K, \alpha)$ yields a SAT/UNSAT transition that is wrong, since it is above the known one for the standard $y = 1$ model. Therefore this scenario should be checked within a 1RSB calculation, where we also expect the dense cluster prediction to remain true. We refer to [12] for an in-depth analysis of a similar model which takes also into account replica symmetry breaking corrections.

Appendix B: Derivation of the lower bound

1. Change of integration variables in second moment bound

The bound in eq. (18) depends on the 8 variables \mathbf{a} . We want now to reduce the number of from 8 to 5 using the constraints in eq. (16). We choose to write a_0, a_6, a_7 as functions of the other variables

$$\begin{cases} a_0 = 1 - a_1 - a_2 - a_3 - x \\ a_6 = x - a_1 - a_2 - a_5 \\ a_7 = a_1 + a_2 - a_4 \end{cases}. \quad (\text{B1})$$

The integration set V_x is then reparametrized as a function of the variables $\vec{a} := (a_1, a_2, a_3, a_4, a_5)$. We indicate with $\mathbf{a}(\vec{a}, x)$ the immersion from \mathbb{R}^5 to \mathbb{R}^8 whose components from a_1 to a_5 are mapped in themselves while the remaining ones are specified by the equations in (B1). This makes the expression of V_x more explicit and lets us rewrite the integral in an equivalent way. The integration set becomes $V'_x \subseteq [0, 1]^5$ and it is specified by the following set of inequalities:

$$\begin{cases} 0 \leq a_i \leq 1 \quad \forall i = 1, \dots, 5 \\ 0 \leq a_1 + a_2 - a_4 \leq 1 \\ a_1 + a_2 + a_5 \leq x \\ a_1 + a_2 + a_3 \leq 1 - x \end{cases}. \quad (\text{B2})$$

With this change of variables eq. (18) becomes:

$$\mathbb{E} \left[\mathcal{Z}_{y=2}^2(x, K, \xi) \right] \leq C_0 N^{3/2} \int_{V'_x} d\vec{a} e^{N[\ln 2 + H_8(\vec{a}, x) + \alpha \ln f_2(\vec{a}, x, K)]}, \quad (\text{B3})$$

where we defined $H_8(\vec{a}, x) := H_8(\mathbf{a}(\vec{a}, x))$ and $f_2(\vec{a}, x, K) := f_2(\mathbf{a}(\vec{a}, x), x, K)$. The covariance matrix in the Gaussian integral $f_2(\vec{a}, x, K)$ is reparameterized in the following way (cf. eq. (13)):

$$\Sigma = \begin{pmatrix} 1 & q_1 & q_{01} & q_{02} \\ q_1 & 1 & q_{03} & q_{04} \\ q_{01} & q_{03} & 1 & q_1 \\ q_{02} & q_{04} & q_1 & 1 \end{pmatrix} \quad \text{where} \quad \begin{cases} q_1 = 1 - 2x \\ q_{01} = 1 - 2(x + a_2 + a_3 - a_4 - a_5) \\ q_{02} = 1 - 2(2a_1 + a_2 + a_3 - a_4 + a_5) \\ q_{03} = 1 - 2(a_2 + a_3 + a_4 + a_5) \\ q_{04} = 1 - 2(x - a_2 + a_3 + a_4 - a_5) \end{cases} \quad (\text{B4})$$

The next and final reparametrization of the integral is suggested by the form of the covariance matrix. In particular we would like to express the four possible overlaps between the two pairs of solution using the four parameters $q_{01}, q_{02}, q_{03}, q_{04}$ and group them in a four dimensional vector \vec{q}_0 . However, since our integration domain is 5-dimensional, we need an additional parameter that we call η . Inverting the under-parametrized system of eqs. (B4), we obtain the vectors \vec{a}^* that lie in the vector space below, for $\eta \in \mathbb{R}$:

$$\begin{cases} a_1^* = \frac{1}{4}(q_{01} - q_{02} + 2x) - \eta \\ a_2^* = \frac{1}{4}(-q_{03} + q_{04} + 2x) - \eta \\ a_3^* = \frac{1}{4}(2 - q_{01} - q_{04} - 4x) + \eta \\ a_4^* = \frac{1}{4}(q_{01} - q_{03} + 2x) - \eta \\ a_5^* = \eta \end{cases} \quad (\text{B5})$$

By constraining the solutions \vec{a}^* in their natural domain V'_x we find how the domain is transformed in the new coordinates \vec{q}_0 and η :

$$\begin{cases} \frac{1}{4}(q_{01} - q_{02} + 2x - 4) \leq \eta \leq \frac{1}{4}(q_{01} - q_{02} + 2x) \\ \frac{1}{4}(-q_{03} + q_{04} + 2x - 4) \leq \eta \leq \frac{1}{4}(-q_{03} + q_{04} + 2x) \\ \frac{1}{4}(q_{01} + q_{04} + 4x - 2) \leq \eta \leq \frac{1}{4}(q_{01} + q_{04} + 4x + 2) \\ \frac{1}{4}(q_{01} - q_{03} + 2x - 4) \leq \eta \leq \frac{1}{4}(q_{01} - q_{03} + 2x) \\ 0 \leq \eta \leq 1 \\ \frac{1}{4}(q_{01} - q_{02} - q_{03} + q_{04}) \leq \eta \\ \frac{1}{4}(-q_{02} + q_{04} + 2x - 4) \leq \eta \leq \frac{1}{4}(-q_{02} + q_{04} + 2x) \\ \frac{1}{4}(-q_{02} - q_{03} + 4x - 2) \leq \eta \end{cases}, \quad (\text{B6})$$

where we have expressed all inequalities in terms of the variable η . This set of inequalities specifies a new integration domain in eq. (B3), this time in the new variables η and \vec{q}_0 , that we call \tilde{V}_x and that depends on x . Again, we can express the vector of solutions \vec{a}^* as a function of the pair (\vec{q}_0, η) . The integral (B3) is rewritten as:

$$\mathbb{E} \left[\mathcal{Z}_{y=2}^2(x, K, \xi) \right] \leq C_0 N^{3/2} \int_{\tilde{V}_x} d\vec{q}_0 d\eta e^{N[\ln 2 + H_8(\vec{q}_0, \eta, x) + \alpha \ln f_2(\vec{q}_0, x, K)]}, \quad (\text{B7})$$

where we adopt the convention that $f_2(\vec{q}_0, x, K) := f_2(\vec{a}^*(\vec{q}_0, \eta), x, K)$ and $H_8(\vec{q}_0, \eta, x) := H_8(\vec{a}^*(\vec{q}_0, \eta), x)$.

2. Proof of Lemma 2

Proof of Lemma 2. From eq. (15) we obtain the following inequalities:

$$\begin{cases} |-a_0 + 1 - a_1 - a_2 - a_3 - x| < \frac{3}{N} \\ |a_6 - x + a_1 + a_2 + a_5| < \frac{1}{N} \\ |a_7 - a_1 - a_2 + a_4| < \frac{2}{N} \end{cases} . \quad (\text{B8})$$

In the limit $N \rightarrow \infty$ these inequalities determine three of the parameters as a function of the other five:

$$\begin{cases} a_0^* = 1 - a_1 - a_2 - a_3 - x \\ a_6^* = x - a_1 - a_2 - a_5 \\ a_7^* = a_1 + a_2 - a_4 \end{cases} . \quad (\text{B9})$$

Notice that the summation on the left hand side of eq. (17) is taken for $\mathbf{a} \in \{0, 1/N, 2/N, \dots, 1\}^8$. If we fix the five components vector $\vec{a} := (a_1, \dots, a_5) \in V'_x \cap \{0, 1/N, 2/N, \dots, 1\}^5$ where V'_x is defined as in eq. (B2), then, independently from this 5-dimensional vector, there exist at most a fixed number of \mathbf{a} 's that satisfy the inequalities in eq. (B8) (for every N and $x \in [0, 1]$). This is sufficient to conclude that for large enough N there exists a positive constant F_0 such that

$$\begin{aligned} \sum_{\mathbf{a} \in V_{N,x} \cap \{0, 1/N, 2/N, \dots, 1\}^8} \binom{N}{Na_0 \dots Na_7} \psi(\mathbf{a})^N &\leq F_0 \sum_{\vec{a} \in V'_x \cap \{0, 1/N, 2/N, \dots, 1\}^5} \binom{N}{\lfloor Na_0^* \rfloor Na_1 \dots Na_5 \lfloor Na_6^* \rfloor Na_7^*} \times \\ &\times \psi(a_0^*, a_1, \dots, a_5, a_6^*, a_7^*)^N . \end{aligned}$$

where V'_x is defined by the system of eqs. (B2).

From Stirling's approximation, the expression for large N and fixed a_i of the multinomial factor is

$$\begin{aligned} \binom{N}{Na_0 \dots Na_m} &= e^{NH(\mathbf{a}) - \frac{m-1}{2} \ln N + O(1)} \\ &\leq G_0 e^{NH(\mathbf{a}) - \frac{m-1}{2} \ln N} \end{aligned}$$

where G_0 is some positive constant and $H(\mathbf{a})$ is the Shannon entropy of the discrete probability distribution with masses $\{a_0, \dots, a_m\}$. Putting all together we have

$$\begin{aligned} &\sum_{\mathbf{a} \in V_{N,x} \cap \{0, 1/N, 2/N, \dots, 1\}^8} \binom{N}{Na_0 \dots Na_7} \psi(\mathbf{a})^N \\ &\leq F_0 \sum_{\vec{a} \in V'_x \cap \{0, 1/N, 2/N, \dots, 1\}^5} \binom{N}{\lfloor Na_0^* \rfloor Na_1 \dots Na_5 \lfloor Na_6^* \rfloor Na_7^*} \psi(a_0^*, a_1, \dots, a_6^*, a_7^*)^N \\ &\leq \frac{F_0 G_0}{N^{\frac{7}{2}}} \sum_{\vec{a} \in V'_x \cap \{0, 1/N, 2/N, \dots, 1\}^5} e^{NH_8(a_0^*, a_1, \dots, a_5, a_6^*, a_7^*) - \frac{7}{2} \ln N} \psi(a_0^*, a_1, \dots, a_5, a_6^*, a_7^*)^N \\ &< C_0 N^{\frac{3}{2}} \int_{V_x} d\mathbf{a} e^{N[H_8(\mathbf{a}) + \ln \psi(\mathbf{a})]} \end{aligned}$$

where we have used the limit of Riemann sums in the last step and $C_0 > F_0 G_0$ is a positive constant that does not depend on N but depends on x . The integral in the last line is defined as in the footnote for Lemma 2. \square

3. Proof of eq. (27)

For finite N we define $\mathcal{N}_2(x)$ and $\mathcal{N}_4(x, \mathbf{a})$ as follows. First,

$$\mathcal{N}_2(x) \equiv \sum_{\{\mathbf{w}^1\}} \sum_{\{\mathbf{w}^2\}} \mathbb{1}\left(d_H(\mathbf{w}^1, \mathbf{w}^2) = \lfloor Nx \rfloor\right),$$

which implies that

$$\begin{aligned} (\mathcal{N}_2(x))^2 &= \left(\sum_{\{\mathbf{w}^1\}} \sum_{\{\mathbf{w}^2\}} \mathbb{1}\left(d_H(\mathbf{w}^1, \mathbf{w}^2) = \lfloor Nx \rfloor\right) \right)^2 \\ &= \sum_{\{\mathbf{w}^1\}} \sum_{\{\mathbf{w}^2\}} \sum_{\{\tilde{\mathbf{w}}^1\}} \sum_{\{\tilde{\mathbf{w}}^2\}} \mathbb{1}\left(d_H(\mathbf{w}^1, \mathbf{w}^2) = \lfloor Nx \rfloor\right) \mathbb{1}\left(d_H(\tilde{\mathbf{w}}^1, \tilde{\mathbf{w}}^2) = \lfloor Nx \rfloor\right). \end{aligned}$$

Then, for $\mathbf{a} \in V_{N,x}$ we have:

$$\begin{aligned} \mathcal{N}_4(x, \mathbf{a}) &\equiv \sum_{\{\mathbf{w}^1\}} \sum_{\{\mathbf{w}^2\}} \sum_{\{\tilde{\mathbf{w}}^1\}} \sum_{\{\tilde{\mathbf{w}}^2\}} \mathbb{1}\left(d_H(\mathbf{w}^1, \mathbf{w}^2) = \lfloor Nx \rfloor\right) \mathbb{1}\left(d_H(\tilde{\mathbf{w}}^1, \tilde{\mathbf{w}}^2) = \lfloor Nx \rfloor\right) \times \\ &\quad \times \mathbb{1}\left(d_H(\mathbf{w}^1, \tilde{\mathbf{w}}^1) = \lfloor N(a_2 + a_3 + a_6 + a_7) \rfloor\right) \mathbb{1}\left(d_H(\mathbf{w}^1, \tilde{\mathbf{w}}^2) = \lfloor N(a_1 + a_3 + a_5 + a_7) \rfloor\right) \\ &\quad \times \mathbb{1}\left(d_H(\mathbf{w}^2, \tilde{\mathbf{w}}^1) = \lfloor N(a_2 + a_3 + a_4 + a_5) \rfloor\right) \mathbb{1}\left(d_H(\mathbf{w}^2, \tilde{\mathbf{w}}^2) = \lfloor N(a_1 + a_3 + a_4 + a_6) \rfloor\right). \end{aligned}$$

From the definitions it follows that $\mathcal{N}_4(x, \mathbf{a}) \leq (\mathcal{N}_2(x))^2$ and computing the summations gives

$$2^N \frac{N!}{\prod_{i=0}^7 (Na_i)!} \leq \left(2^N \binom{N}{\lfloor Nx \rfloor} \right)^2, \quad \forall \mathbf{a} \in V_{N,x} \cap \left\{ 0, \frac{1}{N}, \dots, 1 \right\}^8.$$

Taking the logarithm on both sides, dividing by N and taking the limit for $N \rightarrow \infty$, gives the following inequality

$$\ln 2 + H_8(\mathbf{a}) \leq 2 \log 2 + 2H_2(x) \quad \forall \mathbf{a} \in V_{N,x}.$$

If we apply now the same change of variable of Appendix B 1 the result is

$$H_8(\vec{q}_0, \eta, x) \leq \ln 2 + 2H_2(x) \quad \forall (\vec{q}_0, \eta) \in \tilde{V}_x.$$

4. Numerical optimization

We performed the optimization in expression (32) numerically. We empirically find the objective function to be ridden by many local minima, therefore we implemented 3 different strategies to partition the search space and obtain a numerical estimate of the global one.

A first strategy consists in constructing a 4-dimensional uniformly-spaced grid for the values of \vec{q}_0 , and then performing Gradient Descent (GD) starting from these points and selecting the overall minimum obtained. The downside of this approach is that the optimization is very time-consuming. We simulated grids with up to $m = 100^4$ number of points. We restrict the experiment to the region of small x , in particular $x < x'_c$. The results are shown in fig. 5. While for $x > x'_c$, and already for a

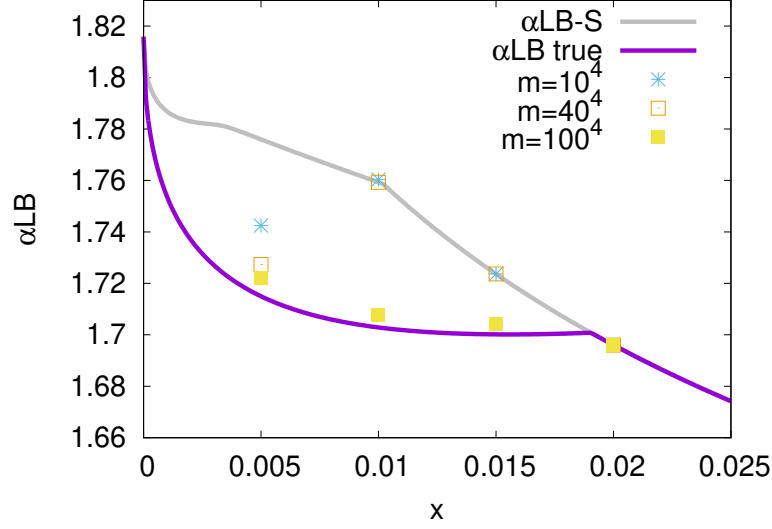


Figure 5. Numerical lower bounds $\alpha_{LB,y=2}(x, K=1)$ obtained by multiple restarts of GD from a 4d grids with m points, for different values of m , along with theoretical predictions from the symmetric point S (that we know to be wrong for $x < x_c$) and the true lower bound (point S for $x > x_c$, point SB for $x < x_c$).

low numbers of points m , the numerical estimate coincides with the symmetric point prediction, for $x < x_c$ instead, where we predict the broken symmetry point to yield the true value of α_{LB} , only with the two finest grid spacing we are able to get close to the theoretical prediction. Overall, the results for this numerical experiment are in good agreement with theoretical value predicted for the saddle point by symmetry arguments, supporting our conclusion that for $x < x_c$ lower and upper bounds coincide.

Another approach is to restrict the search space to a lower dimensional manifold, containing both the symmetric (S) and the symmetry broken (SB) points. The lower dimensionality (2 instead of 4) allows us to use as starting points of our GD procedure grids with smaller spacings. Therefore, we restrict the search space to points of the type $\vec{q}_0 = (q_a, q_b, q_b, q_a)$. The corresponding covariance matrix in this case is given by

$$\Sigma_{SB} = \begin{pmatrix} 1 & q_1 & q_a & q_b \\ q_1 & 1 & q_b & q_a \\ q_a & q_b & 1 & q_1 \\ q_b & q_a & q_1 & 1 \end{pmatrix}. \quad (\text{B10})$$

The optimization over this submanifold is done by multiple restarts of GD from a 2-dimensional grid corresponding of values for q_a and q_b . The results are reported in fig. 6 (Left). Again, while GD quickly finds the global minima for $x > x_c$, the S point, for $x < x_c$ the global minima SB is more difficult to approach, and the restriction to the 2d submanifold doesn't seem to provide a computational advantage, possibly due to the presence of further spurious minima in this restricted space.

A further approach is to just evaluate the objective function in eq. (32) on the points of the increasingly refined 2d-grid, without any GD refinement, and take the lowest of the values obtained. With this approach, we evaluated grids of up to $m = 5000^2$ points. Results are presented in fig. 6 (Right).

All of the 3 approaches are in good agreement with each other and with theoretical predictions.

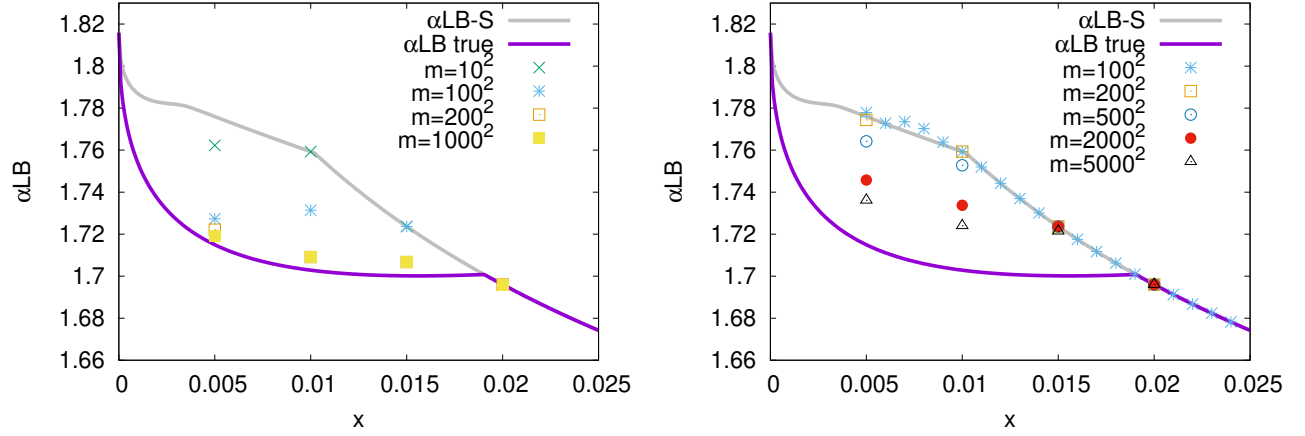


Figure 6. (Left) Numerical and theoretical estimates for $\alpha_{LB,y=2}(x, K=1)$ as in fig. (5) but with GD in 2-dimensional space and multiple restarts from grids of m points. (Right) Evaluation of the points in 2d grids of different sizes m with no GD refinement.

5. Computation of $f_2(\vec{q}_0, x, K)$

The computation in an efficient and precise way of the quantity $f_2(\vec{q}_0, x, K)$ is crucial for the numerical results. We use the Cholesky decomposition of matrix $\Sigma = C_L C_L^T$ where C_L is lower triangular and $C_L^{-1} = C_L^T$. Then it is natural to use the change of variable $\mathbf{y} = C_L^{-1} \mathbf{z}$, in matrix form

$$\begin{pmatrix} z_1 \\ z_2 \\ \tilde{z}_1 \\ \tilde{z}_2 \end{pmatrix} = \begin{pmatrix} c_{11} & 0 & 0 & 0 \\ c_{21} & c_{22} & 0 & 0 \\ c_{31} & c_{32} & c_{33} & 0 \\ c_{41} & c_{42} & c_{43} & c_{44} \end{pmatrix} \begin{pmatrix} y_1 \\ y_2 \\ \tilde{y}_1 \\ \tilde{y}_2 \end{pmatrix}$$

the integral is transformed in the following way:

$$\begin{aligned} f_2(\vec{q}_0, x, K) &= \int_{I_K^4} \frac{dz_1 dz_2 d\tilde{z}_1 d\tilde{z}_2}{(2\pi)^2 |\Sigma|^{1/2}} e^{-\frac{1}{2} \mathbf{z}^T \Sigma^{-1} \mathbf{z}} \\ &= \frac{1}{(2\pi)^2} \int_{-\frac{K}{c_{11}}}^{\frac{K}{c_{11}}} dy_1 \int_{\frac{(-K-c_{21}y_1)}{c_{22}}}^{\frac{(K-c_{21}y_1)}{c_{22}}} dy_2 \int_{\frac{(-K-c_{31}y_1-c_{32}y_2)}{c_{33}}}^{\frac{(K-c_{31}y_1-c_{32}y_2)}{c_{33}}} d\tilde{y}_1 \int_{\frac{(-K-c_{41}y_1-c_{42}y_2-c_{43}\tilde{y}_1)}{c_{44}}}^{\frac{(K-c_{41}y_1-c_{42}y_2-c_{43}\tilde{y}_1)}{c_{44}}} d\tilde{y}_2 e^{-\frac{\mathbf{y}^T \mathbf{y}}{2}} \\ &= \frac{1}{(2\pi)^{\frac{3}{2}}} \int_{-\frac{K}{c_{11}}}^{\frac{K}{c_{11}}} dy_1 \int_{\frac{(-K-c_{21}y_1)}{c_{22}}}^{\frac{(K-c_{21}y_1)}{c_{22}}} dy_2 \int_{\frac{(-K-c_{31}y_1-c_{32}y_2)}{c_{33}}}^{\frac{(K-c_{31}y_1-c_{32}y_2)}{c_{33}}} d\tilde{y}_1 e^{-\frac{y_1^2 + y_2^2 + \tilde{y}_1^2}{2}} \sum_{s=\pm 1} s H\left(\frac{-sK - c_{41}y_1 - c_{42}y_2 - c_{43}\tilde{y}_1}{c_{44}}\right) \end{aligned}$$

where in the last line we have performed the integral over \tilde{y}_2 , using the definition $H(x) = \frac{1}{2} \operatorname{erfc}\left(\frac{x}{\sqrt{2}}\right)$.

Appendix C: n -th moment of y -solutions multiplet using Replica Ansatz

Let us define \mathcal{Z}_y to be the number of configurations of y vectors of binary weights each satisfying the CSP eq. (2) and whose mutual distance is x . In the following we will use the overlap $q_1 = 1 - 2x$ between solutions as an external control parameter. We also introduce for convenience of notation the indicator functions $\varphi_K(z) = \mathbb{1}(|z| \leq K)$ and $\delta(z) = \mathbb{1}(z = 0)$. We denote with δ_D the Dirac's delta distribution. With these definitions we have:

$$\begin{aligned} \mathcal{Z}_y(q_1, K, \xi) &= \sum_{\{\mathbf{w}^a\}_{a=1}^y} \prod_{a=1}^y \mathbb{X}_{\xi, K}(\mathbf{w}^a) \prod_{a < b}^y \delta\left(\sum_i w_i^a w_i^b - \lfloor Nq_1 \rfloor\right) \\ &= \sum_{\{\mathbf{w}^a\}_{a=1}^y} \prod_{a=1}^y \prod_{\mu=1}^M \varphi_K\left(\sum_i w_i^a \xi_i^\mu\right) \prod_{a < b}^y \delta\left(\sum_i w_i^a w_i^b - \lfloor Nq_1 \rfloor\right). \end{aligned}$$

We want to take the expectation of the n -th moment of this partition function:

$$\begin{aligned} \mathcal{Z}_y^n(q_1, K, \xi) &= \sum_{\{\mathbf{w}_\alpha^a\}} \prod_{a, \alpha, \mu} \varphi_K\left(\sum_i w_{\alpha, i}^a \xi_i^\mu\right) \prod_{\alpha, a < b} \delta\left(\sum_i w_{\alpha, i}^a w_{\alpha, i}^b - \lfloor Nq_1 \rfloor\right) \\ &= \sum_{\{\mathbf{w}_\alpha^a\}} \int \prod_{a, \alpha, \mu} d\lambda_{\alpha, \mu}^a \varphi_K\left(\lambda_{\alpha, \mu}^a\right) \delta_D\left(\lambda_{\alpha, \mu}^a - \sum_i w_{\alpha, i}^a \xi_i^\mu\right) \prod_{\alpha, a < b} \delta\left(\sum_i w_{\alpha, i}^a w_{\alpha, i}^b - \lfloor Nq_1 \rfloor\right) \\ &= \sum_{\{\mathbf{w}_\alpha^a\}} \int \prod_{a, \alpha, \mu} \frac{d\lambda_{\alpha, \mu}^a d\hat{\lambda}_{\alpha, \mu}^a}{2\pi} \varphi_K\left(\lambda_{\alpha, \mu}^a\right) e^{i\hat{\lambda}_{\alpha, \mu}^a \lambda_{\alpha, \mu}^a - i\hat{\lambda}_{\alpha, \mu}^a \sum_i w_{\alpha, i}^a \xi_i^\mu} \prod_{\alpha, a < b} \delta\left(\sum_i w_{\alpha, i}^a w_{\alpha, i}^b - \lfloor Nq_1 \rfloor\right). \end{aligned}$$

Now we can take the average over the quenched disorder (in the large N limit, up to the leading exponential order):

$$\begin{aligned} \mathbb{E}[\mathcal{Z}_y^n(q_1, K, \xi)] &= \sum_{\{\mathbf{w}_\alpha^a\}} \int \prod_{a, \alpha, \mu} \left(\frac{d\lambda_{\alpha, \mu}^a d\hat{\lambda}_{\alpha, \mu}^a}{2\pi} \varphi_K\left(\lambda_{\alpha, \mu}^a\right) e^{i\hat{\lambda}_{\alpha, \mu}^a \lambda_{\alpha, \mu}^a}\right) \mathbb{E}\left[e^{\sum_{\mu, i} \xi_i^\mu \sum_{a, \alpha} (-i\hat{\lambda}_{\alpha, \mu}^a w_{\alpha, i}^a)}\right] \prod_{\alpha, a < b} \delta\left(\sum_i w_{\alpha, i}^a w_{\alpha, i}^b - \lfloor Nq_1 \rfloor\right) \\ &\cong \sum_{\{\mathbf{w}_\alpha^a\}} \int \prod_{a, \alpha, \mu} \left(\frac{d\lambda_{\alpha, \mu}^a d\hat{\lambda}_{\alpha, \mu}^a}{2\pi} \varphi_K\left(\lambda_{\alpha, \mu}^a\right) e^{i\hat{\lambda}_{\alpha, \mu}^a \lambda_{\alpha, \mu}^a}\right) e^{-\frac{1}{2N} \sum_{\mu, i} \left(\sum_{a, \alpha} \lambda_{\alpha, \mu}^a w_{\alpha, i}^a\right)^2} \prod_{\alpha, a < b} \delta\left(\sum_i w_{\alpha, i}^a w_{\alpha, i}^b - \lfloor Nq_1 \rfloor\right) \\ &= \sum_{\{\mathbf{w}_\alpha^a\}} \int \prod_{a, \alpha, \mu} \left(\frac{d\lambda_{\alpha, \mu}^a d\hat{\lambda}_{\alpha, \mu}^a}{2\pi} \varphi_K\left(\lambda_{\alpha, \mu}^a\right)\right) e^{i \sum_{\alpha, a, \mu} \hat{\lambda}_{\alpha, \mu}^a \lambda_{\alpha, \mu}^a - \frac{1}{2} \sum_{\mu} \sum_{a, b} \sum_{\alpha, \beta} \hat{\lambda}_{\alpha, \mu}^a \hat{\lambda}_{\beta, \mu}^b \left(\frac{\sum_i w_{\alpha, i}^a w_{\beta, i}^b}{N}\right)} \times \\ &\quad \times \prod_{\alpha, a < b} \delta\left(\sum_i w_{\alpha, i}^a w_{\alpha, i}^b - \lfloor Nq_1 \rfloor\right). \end{aligned}$$

Next, we introduce the overlaps $q_{\alpha\beta}^{ab} = \frac{\sum_i w_{\alpha, i}^a w_{\beta, i}^b}{N}$ via Dirac deltas. :

$$\begin{aligned}
&= \sum_{\{\mathbf{w}_\alpha^a\}} \int \prod_{a,\alpha,\mu} \left(\frac{d\lambda_{\alpha,\mu}^a d\hat{\lambda}_{\alpha,\mu}^a}{2\pi} \varphi_K(\lambda_{\alpha,\mu}^a) \right) \int \prod_{\alpha<\beta;a,b} dq_{\alpha\beta}^{ab} \int \prod_{\alpha,a<b} dq_{\alpha\alpha}^{ab} e^{i \sum_{\alpha,a,\mu} \lambda_{\alpha,\mu}^a \lambda_{\alpha,\mu}^a - \sum_{\mu} \sum_{a,b,\alpha<\beta} \lambda_{\alpha,\mu}^a \lambda_{\beta,\mu}^b q_{\alpha\beta}^{ab}} \times \\
&\quad e^{-\sum_{\mu} \sum_{\alpha,a<b} \lambda_{\alpha,\mu}^a \lambda_{\beta,\mu}^b q_1 - \frac{1}{2} \sum_{\mu} \sum_{a,\alpha} (\lambda_{\alpha,\mu}^a)^2} \prod_{\alpha<\beta;a,b} \delta_D \left(\frac{\sum_i w_{\alpha,i}^a w_{\beta,i}^b}{N} - q_{\alpha\beta}^{ab} \right) \prod_{\alpha,a<b} \delta_D \left(\frac{\sum_i w_{\alpha,i}^a w_{\alpha,i}^b}{N} - q_{\alpha\alpha}^{ab} \right) \delta(N q_{\alpha\alpha}^{ab} - \lfloor N q_1 \rfloor) \\
&\cong \sum_{\{\mathbf{w}_\alpha^a\}} \int \prod_{\alpha<\beta;a,b} \frac{dq_{\alpha\beta}^{ab} d\hat{q}_{\alpha\beta}^{ab}}{2\pi} \int \prod_{\alpha,a<b} \frac{d\hat{q}_{\alpha\alpha}^{ab}}{2\pi} \int \prod_{a,\alpha,\mu} \left(\frac{d\lambda_{\alpha,\mu}^a d\hat{\lambda}_{\alpha,\mu}^a}{2\pi} \varphi_K(\lambda_{\alpha,\mu}^a) \right) \times \\
&\quad \times e^{i \sum_{\alpha,a,\mu} \lambda_{\alpha,\mu}^a \lambda_{\alpha,\mu}^a - \sum_{\mu} \sum_{a,b,\alpha<\beta} \lambda_{\alpha,\mu}^a \lambda_{\beta,\mu}^b q_{\alpha\beta}^{ab} - \sum_{\mu} \sum_{\alpha,a<b} \lambda_{\alpha,\mu}^a \lambda_{\beta,\mu}^b q_1 - \frac{1}{2} \sum_{\mu} \sum_{a,\alpha} (\lambda_{\alpha,\mu}^a)^2} e^{-N \sum_{\alpha<\beta;a,b} \hat{q}_{\alpha\beta}^{ab} q_{\alpha\beta}^{ab}} \times \\
&\quad \times e^{\sum_{\alpha<\beta;a,b} \hat{q}_{\alpha\beta}^{ab} \sum_i w_{\alpha,i}^a w_{\beta,i}^b - N q_1 \sum_{\alpha,a<b} \hat{q}_{\alpha\alpha}^{ab} + \sum_{\alpha,a<b} \hat{q}_{\alpha\alpha}^{ab} \sum_i w_{\alpha,i}^a w_{\alpha,i}^b} \\
&= \int \prod_{\alpha<\beta;a,b} \frac{dq_{\alpha\beta}^{ab} d\hat{q}_{\alpha\beta}^{ab}}{2\pi} \prod_{\alpha,a<b} \frac{d\hat{q}_{\alpha\alpha}^{ab}}{2\pi} e^{N(G_I(q,\hat{q}) + G_S(\hat{q}) + \alpha G_E(q))},
\end{aligned}$$

where we have introduced the interaction, entropic and energetic terms:

$$\begin{aligned}
G_I^{n,y}(q,\hat{q}) &= - \sum_{\alpha<\beta;a,b} \hat{q}_{\alpha\beta}^{ab} q_{\alpha\beta}^{ab} - q_1 \sum_{\alpha,a<b} \hat{q}_{\alpha\alpha}^{ab} \\
G_S^{n,y}(\hat{q}) &= \frac{1}{N} \ln \sum_{\{\mathbf{w}_\alpha^a\}} e^{\sum_{\alpha<\beta;a,b} \hat{q}_{\alpha\beta}^{ab} \sum_i w_{\alpha,i}^a w_{\beta,i}^b + \sum_{\alpha,a<b} \hat{q}_{\alpha\alpha}^{ab} \sum_i w_{\alpha,i}^a w_{\alpha,i}^b} \\
G_E^{n,y,K}(q) &= \frac{1}{\alpha N} \ln \int \prod_{a,\alpha,\mu} \left(\frac{d\lambda_{\alpha,\mu}^a d\hat{\lambda}_{\alpha,\mu}^a}{2\pi} \varphi_K(\lambda_{\alpha,\mu}^a) \right) e^{i \sum_{\alpha,a,\mu} \lambda_{\alpha,\mu}^a \lambda_{\alpha,\mu}^a - \sum_{\mu} \sum_{a,b,\alpha<\beta} \lambda_{\alpha,\mu}^a \lambda_{\beta,\mu}^b q_{\alpha\beta}^{ab}} \times \\
&\quad \times e^{-\sum_{\mu} \sum_{\alpha,a<b} \lambda_{\alpha,\mu}^a \lambda_{\beta,\mu}^b q_1 - \frac{1}{2} \sum_{\mu} \sum_{a,\alpha} (\lambda_{\alpha,\mu}^a)^2}
\end{aligned}$$

We introduce a replica-symmetric ansatz on the matrices $Q_{\alpha\beta}$ and $\hat{Q}_{\alpha\beta}$ which is specified by the following set of equations:

$$Q_{\alpha\beta}^{ab} = \begin{cases} 1 & \text{if } \alpha = \beta \text{ and } a = b \\ q_0 & \text{if } \alpha \neq \beta \\ q_1 & \text{if } \alpha = \beta \text{ and } a \neq b \end{cases} \quad \hat{Q}_{\alpha\beta}^{ab} = \begin{cases} 0 & \text{if } \alpha = \beta \text{ and } a = b \\ \hat{q}_0 & \text{if } \alpha \neq \beta \\ \hat{q}_1 & \text{if } \alpha = \beta \text{ and } a \neq b \end{cases}.$$

In the case $y = 3$ and $n = 2$ they look as follows:

$$Q = \begin{pmatrix} 1 & q_1 & q_1 & q_0 & q_0 & q_0 \\ q_1 & 1 & q_1 & q_0 & q_0 & q_0 \\ q_1 & q_1 & 1 & q_0 & q_0 & q_0 \\ q_0 & q_0 & q_0 & 1 & q_1 & q_1 \\ q_0 & q_0 & q_0 & q_1 & 1 & q_1 \\ q_0 & q_0 & q_0 & q_1 & q_1 & 1 \end{pmatrix} \quad \hat{Q} = \begin{pmatrix} 0 & \hat{q}_1 & \hat{q}_1 & \hat{q}_0 & \hat{q}_0 & \hat{q}_0 \\ \hat{q}_1 & 0 & \hat{q}_1 & \hat{q}_0 & \hat{q}_0 & \hat{q}_0 \\ \hat{q}_1 & \hat{q}_1 & 0 & \hat{q}_0 & \hat{q}_0 & \hat{q}_0 \\ \hat{q}_0 & \hat{q}_0 & \hat{q}_0 & 0 & \hat{q}_1 & \hat{q}_1 \\ \hat{q}_0 & \hat{q}_0 & \hat{q}_0 & \hat{q}_1 & 0 & \hat{q}_1 \\ \hat{q}_0 & \hat{q}_0 & \hat{q}_0 & \hat{q}_1 & \hat{q}_1 & 0 \end{pmatrix}.$$

We now compute the interaction, entropic and energetic terms using this ansatz:

$$G_I^{n,y}(q_0, q_1, \hat{q}_0, \hat{q}_1) = -y^2 \frac{n(n-1)}{2} q_0 \hat{q}_0 - n \frac{y(y-1)}{2} q_1 \hat{q}_1 - \frac{yn}{2} \hat{q}_1 \quad (C1)$$

$$\begin{aligned} G_S^{n,y}(\hat{q}_0, \hat{q}_1) &= \frac{1}{N} \ln \sum_{\{\mathbf{w}_\alpha^a\}} \prod_i e^{\sum_{\alpha < \beta: a, b} \hat{q}_0 w_{\alpha, i}^a w_{\beta, i}^b + \sum_{\alpha, a < b} \hat{q}_1 w_{\alpha, i}^a w_{\alpha, i}^b} \\ &= -\frac{ny\hat{q}_1}{2} + \ln \sum_{\{\mathbf{w}_\alpha^a\}} e^{\frac{1}{2}\hat{q}_0 (\sum_{a\alpha} w_\alpha^a)^2 + \frac{\hat{q}_1 - \hat{q}_0}{2} \sum_\alpha (\sum_a w_\alpha^a)^2} \\ &= -\frac{ny\hat{q}_1}{2} + \ln \sum_{\{\mathbf{w}_\alpha^a\}} \int Dz e^{z\sqrt{\hat{q}_0} \sum_{a\alpha} w_\alpha^a} \int \prod_\alpha Dt_\alpha e^{\sqrt{\hat{q}_1 - \hat{q}_0} \sum_\alpha t_\alpha \sum_a w_\alpha^a} \\ &= -\frac{ny\hat{q}_1}{2} + \ln \int Dz \left[\int Dt \left(2 \cosh \left(\sqrt{\hat{q}_0} z + \sqrt{\hat{q}_1 - \hat{q}_0} t \right) \right)^y \right]^n \end{aligned} \quad (C2)$$

$$\begin{aligned} G_E^{n,y,K}(q_0, q_1) &= \frac{1}{\alpha N} \ln \int \prod_{a, \alpha, \mu} \left(\frac{d\lambda_{\alpha, \mu}^a d\hat{\lambda}_{\alpha, \mu}^a}{2\pi} \varphi_K(\lambda_{\alpha, \mu}^a) \right) e^{i \sum_{\alpha, a, \mu} \hat{\lambda}_{\alpha, \mu}^a \lambda_{\alpha, \mu}^a - \sum_\mu q_0 \sum_{a, b, \alpha < \beta} \hat{\lambda}_{\alpha, \mu}^a \hat{\lambda}_{\beta, \mu}^b} \times \\ &\quad \times e^{-\sum_\mu \sum_{\alpha, a < b} \hat{\lambda}_{\alpha, \mu}^a \hat{\lambda}_{\beta, \mu}^b q_1 - \frac{1}{2} \sum_\mu \sum_{a, \alpha} (\hat{\lambda}_{\alpha, \mu}^a)^2} \\ &= \ln \int \prod_{a, \alpha} \left(\frac{d\lambda_\alpha^a d\hat{\lambda}_\alpha^a}{2\pi} \varphi_K(\lambda_\alpha^a) \right) e^{i \sum_{\alpha, a} \hat{\lambda}_\alpha^a \lambda_\alpha^a - \frac{1}{2} q_0 (\sum_{a\alpha} \hat{\lambda}_\alpha^a)^2 - \frac{q_1 - q_0}{2} \sum_\alpha (\sum_a \hat{\lambda}_\alpha^a)^2 - \frac{1 - q_1}{2} \sum_{a\alpha} (\hat{\lambda}_\alpha^a)^2} \\ &= \ln \int Dz \int \prod_\alpha Dt_\alpha \int \prod_{a\alpha} \left(\frac{d\lambda_\alpha^a d\hat{\lambda}_\alpha^a}{2\pi} \varphi_K(\lambda_\alpha^a) \right) e^{i \sum_{\alpha, a} \hat{\lambda}_\alpha^a \lambda_\alpha^a + iz\sqrt{q_0} \sum_{a\alpha} \hat{\lambda}_\alpha^a + i\sqrt{q_1 - q_0} \sum_\alpha t_\alpha \sum_a \hat{\lambda}_\alpha^a - \frac{1 - q_1}{2} \sum_{a\alpha} (\hat{\lambda}_\alpha^a)^2} \\ &= \ln \int Dz \left[\int Dt \left[\int \frac{d\lambda d\hat{\lambda}}{2\pi} \varphi_K(\lambda) e^{i\hat{\lambda}\lambda + iz\sqrt{q_0}\hat{\lambda} + i\sqrt{q_1 - q_0}t\hat{\lambda} - \frac{1 - q_1}{2}\hat{\lambda}^2} \right]^y \right]^n \\ &= \ln \int Dz \left[\int Dt \left[\int \frac{d\lambda}{\sqrt{2\pi(1 - q_1)}} \varphi_K(\lambda) e^{-\frac{(\lambda + \sqrt{q_0}z + \sqrt{q_1 - q_0}t)^2}{2(1 - q_1)}} \right]^y \right]^n \\ &= \ln \int Dz \left[\int Dt \left[\sum_{s=\pm 1} {}_sH \left(\frac{-sK}{\sqrt{1 - q_1}} + \frac{\sqrt{q_0}z + \sqrt{q_1 - q_0}t}{\sqrt{1 - q_1}} \right) \right]^y \right]^n \end{aligned} \quad (C3)$$

In the last line, as in the main text, the function $H(x)$ is defined as $H(x) \equiv \int_x^\infty Dz \equiv \int_x^\infty \frac{dz}{\sqrt{2\pi}} e^{-z^2/2} = \frac{1}{2} \text{erfc} \left(\frac{x}{\sqrt{2}} \right)$.